Microbial bioindicators of Stony Coral Tissue Loss Disease identified in corals and overlying waters using a rapid field-based sequencing approach

Cynthia C. Becker[1,2], Marilyn Brandt[3], Carolyn A. Miller[1], Amy Apprill[1*]

[1]Woods Hole Oceanographic Institution, Woods Hole, MA, 02543, USA

[2]MIT-WHOI Joint Program in Oceanography/Applied Ocean Science & Engineering, Cambridge and Woods Hole, MA, USA

[3]University of the Virgin Islands, St. Thomas, United States Virgin Islands, 00802, USA

[*]Corresponding author: aapprill@whoi.edu, 508-289-2649, fax – 508-457-2164

Originality-Significance Statement

We developed and integrated a rapid, field-based pipeline for microbiome characterization that uses the smallest Illumina platform, the iSeq 100 System, and applied it to an unprecedented coral disease, Stony Coral Tissue Loss Disease. Here, we present work on microbial bioindicators of this coral disease in the United States Virgin Islands, an area not previously represented in microbial studies of this disease. We also sample for and detect signatures of this coral disease in near-coral seawater (<5 cm of the coral surface), a microbial microenvironment not commonly sampled which may serve as a disease reservoir. By additionally presenting the disease bioindicators in a phylogenetic context, we identify both potential pathogens of the disease and likely novel coral-associated microbes. In addition to identifying specific targets for future work on SCTLD, our framework could be a powerful tool for studying both existing and future marine disease outbreaks.

Abstract

Stony Coral Tissue Loss Disease (SCTLD) is a devastating disease. Since 2014, it has spread along the entire Florida Reef Tract and into the greater Caribbean. It was first detected in the United States Virgin Islands in January 2019. To more quickly identify microbial bioindicators of disease, we developed a rapid pipeline for microbiome sequencing. Over a span of 10 days we collected, processed, and sequenced coral and near-coral seawater microbiomes from diseased and apparently healthy *Colpophyllia natans*, *Montastraea cavernosa*, *Meandrina meandrites* and *Orbicella franksi*. Analysis of bacterial and archaeal 16S ribosomal RNA gene sequences revealed 25 bioindicator amplicon sequence variants (ASVs) enriched in diseased corals. These bioindicator ASVs were additionally recovered in near-coral seawater (<5 cm of coral surface), a potential reservoir for pathogens. Phylogenetic analysis of microbial bioindicators with

sequences from the Coral Microbiome Database revealed that *Vibrio, Arcobacter,* Rhizobiaceae, and Rhodobacteraceae sequences were related to disease-associated coral bacteria and lineages novel to corals. Additionally, four ASVs (*Algicola*, *Cohaesibacter*, *Thalassobius* and *Vibrio*) were matches to microbes previously associated with SCTLD that should be targets for future research. Overall, this work suggests that a rapid sequencing framework paired with specialized databases facilitates identification of microbial disease bioindicators.

1. INTRODUCTION

Stony Coral Tissue Loss Disease (SCTLD) is a rapidly progressing, persistent, and widespread coral disease that affects at least 24 reef-building coral species in the Caribbean (Florida Keys National Marine Sanctuary, 2018). Since 2014, when it was first detected off Miami-Dade county, FL, it has devastated Floridian reefs, where loss in live coral has been as high as 60% (Precht *et al.*, 2016; Walton *et al.*, 2018). In the following years, the disease spread over the entire Florida Reef Tract and in 2018, the disease had appeared in disparate areas of the Caribbean (Kramer *et al.*, 2021). The SCTLD outbreak is one of the longest and most widespread coral disease outbreaks ever to be recorded (Rosales *et al.*, 2020). The extended duration, widespread occurrence, and high species susceptibility associated with SCTLD make this an unprecedented and devastating coral disease.

When SCTLD first emerged on Floridian reefs, it initially impacted species including *Meandrina meandrites, Dichocoenia stokesii, Dendrogyra cylindrus* (an Endangered Species Act-listed coral), and the brain corals (i.e. *Colpophyllia natans, Pseudodiploria strigosa*). In ensuing months after the initial outbreak, other species began to show signs of SCTLD, including bouldering-type corals such as *Montastraea cavernosa,* and *Orbicella* spp. (Florida Keys National Marine Sanctuary, 2018). Similar assemblages of affected species and disease ecology

confirmed the emergence of SCTLD on reefs off of Flat Cay, an unoccupied island off of St. Thomas, U.S. Virgin Islands (USVI), in January 2019. Tissue loss on USVI corals progress at rates up to 35-fold higher than other common coral diseases and leads to complete mortality of over half of afflicted colonies (Meiling *et al.*, 2020). Throughout 2019, and until the time of sampling in February 2020, the disease spread around the island of St. Thomas and east to the island of St. John (VI-CDAC, 2021).

The causative agent(s) responsible for SCTLD remain elusive, a common feature of the majority of coral diseases (Mera and Bourne, 2018; Vega Thurber *et al.*, 2020). Further, the lack of correlation between SCTLD severity and ambient temperature or chlorophyll concentrations, suggests that a novel, yet highly contagious, pathogen may be responsible (Muller *et al.*, 2020). Successful cessation of lesion progression following application of amoxycillin paste to afflicted colonies suggests that either the pathogen(s) are of bacterial origin or that bacteria play a role in disease progression and virulence as opportunistic microbes (Aeby *et al.*, 2019; Neely *et al.*, 2020). To detect disease bioindicators, 16S ribosomal RNA (rRNA) gene sequencing approaches that target bacteria and archaea were employed on field-collected coral samples from the Florida Reef Tract, where the disease originated (Meyer *et al.*, 2019; Rosales *et al.*, 2020). Meyer and colleagues (2019) found bacteria from five genera, including *Vibrio, Arcobacter, Algicola, Planktotalea,* and one unclassified genus that were consistently enriched in the lesion tissue of three species (*Montastraea cavernosa*, *Diploria labyrinthiformis* and *Dichocoenia stokesii*). In a separate study (Rosales *et al.*, 2020), Rhodobacterales and Rhizobiales sequences were associated with lesions in *Stephanocoenia intersepta*, *D. labyrinthiformis*, *D. stokesii* and *Meandrina meandrites*. It remains to be seen if these same microbial taxa are associated within

SCTLD lesions across the greater Caribbean, especially in the geographically distant USVI, as well as in other coral species affected by the disease.

With such a widespread occurrence, it is important to understand the ways in which SCTLD is transmitted. It is hypothesized that transmission of this disease is through the water column, as evidenced by tank-based experiments (Aeby *et al.*, 2019) and modeling of likely dead coral material and sediments within neutrally buoyant water parcels (Dobbelaere *et al.*, 2020). Additionally, disease-associated microbial taxa were recovered in water and sediment of diseased-afflicted coral reefs, indicating that sediment may also play a role in transmission (Rosales *et al.*, 2020). Disease-associated taxa or putative pathogens have yet to be examined in seawater directly surrounding diseased coral colonies using a targeted sampling method, such as syringe-based water sampling over corals (Weber *et al.*, 2019).

The seawater directly overlying coral, here termed "near-coral seawater", is an important reef environment. Compared to surrounding reef seawater, this environment is characterized by microbes with unique metabolisms and more virulent-like and surface-associated lifestyles (Weber *et al.*, 2019). Also, this near-coral seawater environment is hypothesized to be a recruitment zone for both symbiotic microorganisms and potential pathogens (Weber *et al.*, 2019). While coral physiology may influence the microbes living in this environment, water flow and surrounding currents also play a role (Silveira *et al.*, 2017). Given existing evidence and hypotheses that the SCTLD pathogen or pathogens are water-borne (Aeby *et al.*, 2019; Dobbelaere *et al.*, 2020; Rosales *et al.*, 2020), directly targeting the zone of potential pathogen recruitment is important for supporting these claims.

The rapid spread, persistence, and virulence of SCTLD make it imperative to develop speedier response procedures for understanding this disease. While microbial community

profiling cannot verify candidate pathogens, it is one step in the process of elucidating SCTLD causation through identification of microbial indicators that can be tested further for their role in disease etiology. Additionally, these methods offer a breadth of information, but can fall short in processing time. Typical microbiome pipeline procedures involve weeks to months of sample processing, sequencing, and data analysis. Combined with the requirement for specialized equipment, these procedures are often difficult to conduct in remote island reef locations. Field-based sequencing circumvents these challenges and offers additional benefits, such as working immediately with fresh samples, and in the case of marine disease studies, the quickly processed data could even inform sampling strategies during the timeline of the project (Apprill, 2019). Recently, Illumina Inc. developed the iSeq 100 System, a portable sequencing platform. The platform uses sequencing by synthesis chemistry combined with complementary metal-oxide semiconductor (CMOS) technology and produces 8 million reads, with greater than 80% of reads passing a quality score of Q30 (99.9% base call accuracy) in each run (Illumina, Inc., 2020). Additionally, the CMOS technology allows the sequencing to occur all in a small, single-use cartridge, contributing to its ease of use in mobile (e.g., ship) laboratory settings. More portable sequencing technology and the increasing availability of portable thermocycler machines and centrifuges have made it possible to set up molecular laboratories in almost any environment with an electrical connection.

Here, we developed and applied a rapid coral microbiome sequencing pipeline designed to more quickly gather data on the effects of SCTLD currently affecting numerous nations and reefs across the Caribbean. By setting up small, portable molecular biology tools in a home rental, we successfully collected, processed, and sequenced diseased and apparently healthy coral and near-coral seawater samples at two reefs in St. Thomas, USVI (Fig. 1). We were interested in

answering the following questions regarding the implementation of this rapid pipeline to more broadly understand the etiology of SCTLD: (1) How effective is a portable sequencing approach for coral disease studies, and potentially other marine diseases, (2) What microbial taxa are differentially distributed in healthy and diseased coral, and which may be bioindicators of the disease, (3) Can we identify SCTLD bioindicator microbes in the seawater directly overlying healthy and diseased corals, and (4) To what extent are these SCTLD bioindicators phylogenetically related to known or unknown coral-associated bacteria?

2. RESULTS

2.1 Output of field-based sequencing in a portable microbiome laboratory

Three field-based sequencing runs with the Illumina iSeq 100 system each generated about 2 GB of paired-end, 150 bp sequencing data. In total, 12,997,634 sequencing reads were produced and used for subsequent data analysis. Each sequencing run lasted approximately 17 hours, and the runs were conducted on sequential days from February18th to 20th, 2020. The three days of sequencing produced high quality reads, with the forward reads containing 89.6%, 94.8%, and 89.8% of reads having a Q30 score or better, respectively. Following filtration of forward sequencing reads, the number of reads for the 49 coral samples ranged from 60,105 to 128,036, with an average of 99,177 (± 14,511) while the range for the 51 seawater samples was 68,527 to 119,141, with an average of 96,933 (± 10,218) (Table S2). Thus, all samples were successfully sequenced with sufficient sequence reads for downstream analysis (60,000+ sequences). The average numbers of sequences recovered from the controls were as follows (average ± 1SD, n): Syringe method control samples (96,290 ± 7,542, n = 9), DNA extraction control samples (19,418 ± 11,672, n = 6), and PCR negative control samples (9,930 ± 904, n = 3) (Table S2).

Over the course of the three sequencing runs, the same mock community of 20 known bacteria was sequenced to verify consistency and success of sequencing and ASV generation over the three individual runs. Successful identification of all 20 exact amplicon sequence variants within the mock community was achieved from all three runs, though for each, additional sequence variants were also recovered.

2.2 Health state determines coral microbiome structure while near-coral seawater microbiomes change according to site

Visualization of microbial beta diversity in corals using Principal Coordinates analysis (PCoA) of Bray-Curtis dissimilarity revealed significant changes in the coral microbiota associated with health condition, coral species, and reef site (Fig. 3a, Fig. S1-S2, Table 1). Permutational Analysis of Variance (PERMANOVA) tests comparing diseased ("DD"; n = 21) to healthy pooled from two sample types (healthy from diseased colonies, "HD", and healthy from healthy colonies, "HH"; pooling occurred because samples from apparently healthy colonies from all species was not available; n = 28) revealed disease state as having a significant effect on coral microbiome composition (Fig. 3a, $R^2 = 0.25$, $p < 0.001$). The effect of health state, irrespective of species, was slightly higher when split up by all three conditions ("HH", "HD", "DD", Fig. 3a, PERMANOVA, $R^2 = 0.26$, $p<0.001$). The effect of species on structuring coral microbial communities was also significant, though the effect size was smaller than between healthy and diseased corals (Fig. 3a, Fig. S1-S3, PERMANOVA, $R^2 = 0.15$, $p<0.001$). Interestingly, a PERMANOVA with disease state nested within coral species exerted an even greater effect, explaining 36% of microbiome structure (Fig. 3a, $R^2 = 0.36$, $p<0.001$). Together, disease state, species, and the nested designation exerted a larger effect on the microbial community composition compared to site-based changes between Buck Island (n = 30) and

Black Point (n = 19), though site did significantly structure the coral microbial communities (Fig. 3a, Fig. S2-S3, Table 1, PERMANOVA, $R^2 = 0.041$, $p = 0.031$). Only two coral species, *C. natans* and *M. cavernosa,* were sampled at both Buck Island and Black Point. A PCoA of Bray-Curtis dissimilarity and subsequent PERMANOVA test on only those two species revealed site to be an insignificant factor in structuring the microbiome (Fig S2, PERMANOVA, $R^2 = 0.04$, $p = 0.166$), compared to health state ("HH" and "HD" vs. "DD")(Fig S2, PERMANOVA, $R^2 = 0.31$, $p<0.001$).

Analysis of dispersion of beta diversity revealed significant differences between coral health states (healthy vs. diseased) (Fig. 3b). The distance to centroid of all healthy corals (HH and HD) was significantly lower, though more variable, than that of diseased corals (independent Mann-Whitney U Test, $p < 0.001$, Fig. 3b). Diseased microbiome beta diversity dispersion was higher and more consistent compared to healthy microbial beta diversity (Fig. 3b). Healthy coral microbiomes were generally less dispersed (more closely clustered in the PCoA) except for a few samples, which were dispersed farther from the other healthy samples (Fig. 3a,b). Furthermore, the range in raw Bray-Curtis dissimilarity values within each coral sample (healthy vs. diseased), reinforced the finding of increased beta diversity dispersion of diseased compared to healthy corals (Mann-Whitney U Test $p < 0.001$, Fig. S4).

The effect of disease state was also visible in the stacked bar plot of coral microbiomes (Fig. S5). Notably, *M. cavernosa* contained increased relative abundances of Deltaproteobacteria in diseased corals (Fig. S5b). *Clostridia* and *Campylobacteria* relative abundances were increased in diseased corals, though *Clostridia* was most prominent in diseased *M. cavernosa* and *C. natans*, while *Campylobacteria* was most prominent in diseased *O. franksi.* (Fig. S5).

193 Interestingly, Oxyphotobacteria (predominantly *Prochlocococcus* and *Synechococcus*) decreased
194 in relative abundance in diseased coral (Fig. S5).

195 Near-coral seawater microbiomes (n = 51, Table 1) taken within 5 cm of the coral
196 surface were clearly distinct from coral microbiomes (n = 49, Table 1), but structured according
197 to site (PERMANOVA $R^2 = 0.67$, $p < 0.001$) and not disease state (PERMANOVA $R^2 = 0.005$, p
198 = 0.921) (Fig. 3c, Fig. S1). Coral species also significantly affected the composition of the
199 overlying seawater (Fig. 3c, PERMANOVA, $R^2 = 0.22$, $p = 0.004$).

200 **2.3 Coral disease bioindicators**

201 To detect potential bioindicators of SCTLD, we used the beta-binomial regression model
202 of the *corncob* R package (Martin *et al.*, 2020) to test for differentially abundant ASVs between
203 healthy (HH and HD) and diseased (DD) corals individually for each species (Table 1 for sample
204 replication). The model recovered 25 ASVs that were significantly more abundant, i.e. enriched
205 and herein referred to as bioindicators, in the diseased sample of at least one of the coral species
206 (Fig. 4, Table S3, Fig. S6-S9). Ten of those 25 ASVs were enriched in diseased samples of more
207 than one coral species but none were enriched in all species (Table S3, Fig. S6-S9). Nonetheless,
208 some ASVs, such as ASV44 (*Fusibacter*), were enriched in diseased coral from all species,
209 though the trend was not always significant. The 25 bioindicator ASVs classified as belonging to
210 12 Families and 14 genera. Families with multiple bioindicator ASVs were Arcobacteraceae,
211 Desulfovibrionaceae, Family XII of the order Clostridiales, Rhodobacteraceae, and Vibrionaceae
212 (Table S3). Within these, four ASVs belonged to the genera *Arcobacter*, five to *Vibrio*, and three
213 to *Fusibacter*.

214 In addition to identifying ASVs enriched in diseased coral, the differential abundance
215 analysis revealed other ASVs that were depleted in diseased relative to healthy samples, and

were therefore healthy coral-associated (coefficient < 0, Fig. S6-S9). *M. meandrites* had only one ASV enriched in healthy samples (Family Terasakiellaceae from Rhodospirillales; Fig. S9). Healthy samples of *C. natans* (Fig. S6) and *M. cavernosa* (Fig. S7) were enriched with ASVs belonging to Clades Ia, Ib, and unclassified Clade II of SAR11, the NS4 Marine Group and NS5 Marine Group of Flavobacteriaceae, *Prochlorococcus* MIT9313*, Synechococcus* CC9902, and unclassified SAR116. Healthy *C. natans* also was enriched in ASVs belonging to unclassified Rhodobacteraceae, Clade 1a Lachnospiraceae, and OM60 (NOR5) clade of Halieaceae. Unique healthy-associated ASVs in *M. cavernosa* included 11 diverse taxa (Fig. S7). Healthy coral-associated ASVs from *O. franksi* largely represented taxa found in healthy corals from at least one of the other species targeted in this study (Fig. S8). One unclassified Arcobacteraceae ASV was associated with healthy *O. franksi*, as well as two *Endozoicomonas* ASVs (ASV99, ASV108).

2.4 Disease bioindicator taxa recovered within near-coral seawater

Previous studies indicated that seawater may be a vector for the SCTLD pathogen(s); therefore, we hypothesized that the seawater within 5 cm of coral lesions would harbor the 25 SCTLD bioindicator ASVs we identified from corals. A differential abundance test of the 25 bioindicator ASVs in seawater overlying disease lesions (DD, n = 22, Table 1) compared to healthy corals (HH and HD, n = 29, Table 1) did not find significant enrichment of those ASVs in seawater over diseased lesions. We further tested the 25 bioindicator ASVs in near-coral seawater over apparently healthy colonies compared to disease lesion colonies of *M. cavernosa,* the only species for which we had sufficient replication of apparently healthy colonies and found no ASV significantly enriched in waters overlying diseased corals. Despite the lack of significant enrichment of putative pathogens within near-coral lesion seawater, we did observe all 25

bioindicator ASVs in the near-coral seawater over diseased corals, except for two ASVs (*Cohaesibacter* ASV226 and *Desulfovibrio* ASV185). Several of the SCTLD-associated ASVs were present in seawater overlying all four diseased coral species, including *Algicola* (ASV52), *Arcobacter* (ASV21, ASV101), *Halodesulfovibrio* (ASV13), *Marinifilum* (ASV39), and *Vibrio* (ASV20) (Fig. 5). Interestingly, ASV34, an unclassified Rhodobacteraceae, was found only in near-coral seawater directly overlying disease lesions, but not over healthy corals across all species (Fig. 5). Overall, disease-enriched bacteria were identified at low levels (<1.5% relative abundance) in near-coral seawater, though there was no significant enrichment of these taxa over diseased coral.

2.5 Phylogenetic analysis of SCTLD-enriched taxa

Given the high representation of *Arcobacter*, *Vibrio,* Rhizobiaceae and Rhodobacteraceae ASVs in the bioindicator ASVs, we produced phylogenetic trees to better predict species-level identifications and to relate the ASVs to other sequences associated with coral disease, sequences from the Coral Microbiome Database (Huggett and Apprill, 2019) and SCTLD-associated ASV sequences reported from two previous studies (Meyer *et al.*, 2019; Rosales *et al.*, 2020). Phylogenetic analysis of the Campylobacterota (formerly Epsilonbacteraeota) genus *Arcobacter* spp. indicated no close relationship of the SCTLD-associated ASVs to described *Arcobacter* isolates. Instead, all SCTLD-associated ASVs grouped in clades with coral-associated or coral disease sequences (Fig. S10).

Phylogenetic analysis of the SCTLD bioindicator ASVs from the gammaproteobacterial genus *Vibrio* leveraged a reference tree previously constructed using existing coral-associated sequences found in the Coral Microbiome Database (Huggett and Apprill, 2019), *Vibrio* type strains and a SCTLD-associated *Vibrio* ASV by Meyer and colleagues (2019). ASV20 displayed

high sequence identity to *V. harveyi* ATCC 35084, an isolate obtained from a brown shark kidney following a mortality event (formerly known as *V. carchariae* (Grimes *et al.*, 1984; Pedersen *et al.*, 1998) (Fig. S11). Interestingly, *Vibrio* ASV54 in the present study was an exact sequence match to a longer (253 bp) SCTLD-associated ASV reported previously (Meyer *et al.*, 2019), and this sequence is novel to corals (Table 2, Fig. S11). The remaining bioindicator ASVs 96, 67, and 25 all displayed high sequence identity to other coral-associated *Vibrio* sequences (Fig. S11).

We produced a phylogenetic tree with all known SCTLD-associated ASVs that classified to Rhizobiaceae, sequences from other coral disease studies, and other related sequences (Fig. S12). One bioindicator ASV from the present study (ASV226) was identical in the 126 bp overlapping region to a previous SCTLD-associated ASV11394 (Rosales *et al.*, 2020), and both grouped with *Cohaesibacter marisflavi*, a bacterium that has been isolated from seawater (Table 2, Fig. S12). ASV18209 and ASV19474 also fell within the *Cohaesibacter* genus, close to sequences isolated from White Plague-affected corals (Fig. S12). SCTLD-associated ASV19959, ASV30828, and ASV16110 from Rosales *et al.* (2020) were most closely related to *Pseudovibrio denitrificans* NRBC 100300 (Fig. S12). Finally, the unclassified Rhizobiaceae ASV34211 and ASV24311 (Rosales *et al.*, 2020) were closely associated to isolates of *Hoeflea* spp. and *Filomicrobium* spp., respectively (Fig. S12).

Phylogenetic analysis of SCTLD bioindicators that classified as Rhodobacteraceae using a reference tree generated from the Coral Microbiome Database (Huggett and Apprill, 2019) revealed close classification to bacteria associated with coral hosts that were distinct from existing isolates (Fig. S13). Several SCTLD-associated ASVs from Rosales and colleagues (2020) (ASV15252, ASV24736, ASV13497, ASV3538, and ASV29944) were related to

sequences from ballast water and hypersaline mats rather than coral sequences (Fig. S13). In contrast, the SCTLD bioindicator ASV60 from the present study had high sequence identity to other coral-associated Rhodobacteraceae sequences with no definitive classification, though related to *Phaeobacter* (Fig. S13). Several Rhodobacteraceae ASVs classified to *Thalassococcus* sequences (ASV29894, ASV25482, ASV29283 from Rosales *et al.* (2020)) and ASV111 from the present study (exact sequence match to ASV29283 from Rosales *et al.* (2020)). Finally, SCTLD-associated ASV34 classified within the likely *Marinovum* genus alongside many coral-associated sequences (Fig. S13).

3. DISCUSSION

To better understand the effect of Stony Coral Tissue Loss Disease on coral reefs in the U.S. Virgin Islands, an area with an active and detrimental SCTLD outbreak (VI-CDAC, 2021), we developed and integrated a rapid, field-based 16S rRNA gene sequencing approach to characterize microbiomes of coral and near-coral seawater of SCTLD-infected colonies. St. Thomas, USVI does not have a molecular ecology laboratory or sequencing facility; therefore, we transformed a home rental on the island to a molecular laboratory, and in the span of two weeks, we carried out a complete microbiome workflow, from sample collection to sequencing. This short timeline enabled us to process fresh samples, gather data more quickly, and begin data analysis in the following months, which revealed significant differences between healthy and diseased coral, regardless of coral species or reef location. Differential abundance analysis identified 25 SCTLD bioindicators, all of which were present in the seawater directly overlying coral. Furthermore, these bioindicator ASVs represented sequences with high sequence identity

to the 16S sequence of the *Vibrio harveyi* pathogen, as well as sequences previously identified in diseased corals.

3.1. SCTLD lesion microbial communities are unique from healthy microbial communities

We identified clear and consistent differences between healthy and diseased coral microbiomes, regardless of location and species of coral. In addition, the dispersion of beta-diversity was consistently higher among the diseased corals, compared to all healthy corals, which had reduced, yet more variable dispersion of beta diversity. This greater beta diversity across diseased coral microbiomes could be indicative of some level of microbial dysbiosis associated with disease (MacKnight *et al.*, 2021). Alternatively, the syringe-based collection method results in a homogenate of newly compromised, diseased tissue, as well as necrotic or sloughed off tissue that likely captures potential pathogen(s), organisms involved in secondary infections, or even saprophytic microorganisms proliferating off the exposed skeleton and dead coral tissue (Burge *et al.*, 2013; Egan and Gardiner, 2016). For example, the finding of increased Deltaproteobacteria in diseased samples of *M. cavernosa,* and the significant enrichment of *Halodesulfovibrio,* known sulfate-reducing bacteria, may have been a signature of the exposed coral skeleton (Chen *et al.*, 2019), or perhaps anaerobic degradation of coral tissue (Viehman *et al.*, 2006). Overall, the finding that disease impacts coral microbiome structure in the USVI is supported by previous findings that show shifts in coral microbiomes between healthy and diseased corals in Florida, USA (Meyer *et al.*, 2019; Rosales *et al.*, 2020).

While this study did not identify causative agents of SCTLD, the differential abundance analysis between healthy and diseased coral microbial communities revealed 25 disease bioindicator ASVs, which may represent potential pathogens or opportunistic bacteria relevant for future experimental work. Of these, we identified one ASV (ASV20), with 100% similarity

in the overlapping region to *V. harveyi* (EU130475.1), a pathogen isolated from a shark mortality event, and shown to be virulent for spiny dogfish (*Squalus acanthias*) (Grimes *et al.*, 1984). This ASV was consistently detected in diseased coral (DD samples), including all *C. natans, M. meandrites* and *O. franksi* colonies, and two-thirds of the *M. cavernosa* colonies, at relative sequence abundances of 5% or lower. Additionally, this ASV was frequently recovered in the HD and HH colonies, and most near-coral seawater samples, indicating its broad prevalence in these diseased reefs. Interestingly, *V. harveyi* has been suggested as the causative agent of white syndrome disease in aquaria and field-based corals (Luna *et al.*, 2010). Despite the prevalence of *V. harveyi* sequences in the present SCTLD study, this was not a SCTLD-associated bacterium identified in the Florida-based studies. Still, it seems relevant to examine pathogenicity of *V. harveyi* in future coral disease experiments.

Four of our SCTLD bioindicator ASVs were identical to ASVs identified in Florida-based SCTLD studies. *Algicola* ASV52 and *Vibrio* ASV54 were identical to ASVs identified in Florida by Meyer *et al.* (2019). These sequences have been associated with coral disease in the past (black band disease or white plague disease type II; reviewed by Meyer *et al.* 2019), but were phylogenetically distinct from other known coral-associated lineages (Fig. S11). Furthermore, although not significant in all coral species, the noticeable enrichment in abundance of both ASV52 (*Algicola*) and ASV54 (*Vibrio*) in corals may be biologically relevant, given their association with SCTLD-affected corals sampled in Florida approximately 1,800 km away (Meyer *et al.*, 2019).

Two other bioindicator ASVs in the present study, *Cohaesibacter* (ASV226) and *Thalassobius* (ASV111), matched identical regions of ASVs enriched in a study of Florida-based SCTLD-associated microbiomes by Rosales et al. (2020). In our study, *Cohaesibacter* ASV226

was enriched in diseased *O. franksi,* but barely detected in other corals. Rosales *et al.* (2020) detected the same ASV in *S. intercepta, D. labyrinthiformis,* and *M. meandrites* affected by SCTLD. Phylogenetic analysis placed those two similar sequences (ASV226 and ASV11394, Fig. S12) with *Cohaesibacter marisflavi*, a species not currently known to be a pathogen (Qu *et al.*, 2011). Although no *Cohaesibacter* species are known pathogens, *C. intestini* was isolated from the intestine of an abalone (Liu *et al.*, 2019). Two *Cohaesibacter* sequences identified by Rosales *et al.* (2020) were related to sequences previously isolated in cases of coral disease, indicating *Cohaesibacter* may be an important target for future study. Additionally, *Thalassobius* (ASV111) was an exact match to one of eight Rhodobacteraceae ASVs enriched in diseased corals in the Rosales *et al.* (2020) study. In the present study, this ASV was significantly enriched only in *C. natans,* but was generally present in all diseased corals. Furthermore, these ASVs, and two other disease-associated ASVs (ASV29894 and ASV25482) from Rosales *et al.* (2020) classified as unique unclassified coral bacteria and coral white plague disease afflicted, respectively. Interestingly, several of the SCTLD-associated ASVs added into the Rhodobacteraceae phylogenetic tree were more closely associated to sequences from hypersaline mat or ballast water environments than coral-associated sequences. Despite variability in putative identity of the diverse Rhodobacteraceae sequences associated with SCTLD, exact sequences recovered from diseased corals across geographic regions in the Caribbean (Florida, USA, and USVI) may indicate some concordance in the effect of this disease on different coral species regardless of geography.

It should be noted that there are some methodological differences between the SCTLD studies, which could impact the microbial sequences recovered and compared. The studies all utilized the same primers, but the sequencing platforms differed in read length; the previous

studies used merged reads, enabling a total read length of approximately 253 bp, whereas this study used 126 bp forward reads due to sequencing of primers. Although our amplicons are shorter and we only used forward reads, classification and taxonomic certainty does not decrease linearly with amplicon size, and may be between 71.1-83.2% accurate at the genus level compared to full length small subunit rRNA sequences (Wang *et al.*, 2007) and even up to 99% confident at the phylum level compared to the approximately 253 bp V4 region targeted by the 515F and 806R primers (Liu *et al.*, 2020). Despite this, it should be noted that identical 16S rRNA sequences do not always indicate identical species or genera, when analyzed at the whole genome level (Stackebrandt and Goebel, 1994). All three studies compared here employed the DADA2 analysis pipeline, resulting in sequences published alongside ASV identifiers, allowing for comparison of amplicon sequence variants across studies, a significant benefit of the DADA2 pipeline (Callahan *et al.*, 2017). Lastly, we did take care to insert the shorter amplicon sequences into a phylogenetic framework based on longer read sequences. Overall, the placement of the ASVs appear robust, but additional marker genes or genomes are necessary to confirm the taxonomies affiliated with the ASV-based sequences.

Similar to previous reports for white plague disease, it could be that both bacteria and viruses play a role in SCTLD onset and virulence. Antibiotic pastes containing amoxicillin have been shown to be effective at slowing and halting progression of SCTLD (Aeby *et al.*, 2019; Neely *et al.*, 2020). Despite this, we cannot rule out the role of viruses in this disease, which have been shown to play a role in white-plague-like diseases (Soffer *et al.*, 2014). We did not investigate viruses in our study, but metagenomic and microscopic techniques that investigate holobiont components, such as bacteria, archaea, DNA and RNA-based viruses, and fungi, should be employed in the future. Finally, due to limited availability, this study lacks replication

of samples from apparently healthy colonies ("HH") and future work could aim to prioritize collection of samples from apparently healthy colonies, as it would serve as an important baseline for comparison.

3.2. Signals of SCTLD infection in near-coral seawater

Bioindicator microbes identified as SCTLD-enriched were broadly recoverable in near-coral seawater (<5 cm) surrounding the coral colonies, in agreement with a current hypothesis that seawater is the disease vector (Aeby *et al.*, 2019). However, seven ASVs were found in fewer than five of the nine samples. According to the differential abundance comparison, none of the disease bioindicator ASVs were significantly enriched in seawater overlying diseased compared to healthy areas of the corals, though the relative closeness (<30 cm) between healthy and diseased seawater samples may have mixed this signal. The largest driver of differences in near-coral seawater microbial communities was location. The two reefs we sampled were distinct reefs approximately 12 km away from each other and featured overall similar environmental conditions (Table S1).

Beyond seawater, recent evidence suggests that sediments surrounding coral may play an important role as a reservoir of SCTLD pathogens (Rosales *et al.*, 2020) though that was not sampled here. Future investigations into SCTLD vectors should aim to sample both near-coral sediments and seawater, both *in situ* and in isolated mesocosm tanks to provide further information on the likely modes of transmission of SCTLD pathogens.

3.3. Rapid and portable microbiome profiling is feasible and applicable to marine diseases

Here we successfully implemented an in-the-field microbiome protocol to rapidly gather data on microbiome composition associated with the destructive coral disease, SCTLD. Illumina launched the iSeq 100 System only recently, in 2018. It is the smallest (1 foot cube), cheapest,

and most portable Illumina technology to date and features a single-use cartridge that houses all sequencing reagents, further contributing to its ease of use. Following three sequencing runs, the number of reads generated by the iSeq per sample was comparable to those recovered in a previous study of SCTLD microbiomes that used MiSeq sequencing for the same region of DNA and the same sample collection method (Meyer *et al.*, 2019). Overall, the Illumina iSeq 100 System could be an ideal target for future studies on marine disease outbreaks, when there is a need for rapid information and results to better inform remediation and management of such disease outbreaks.

The present workflow could be applied again to SCTLD research, with some improvements. Although the data were gathered within 10 days of the project start, data analysis still took months. To circumvent this, all data analysis scripts are saved and easily accessible on GitHub, so future data could be easily processed and compared to the present findings. Additional work could focus on producing data analysis scripts that incorporate predictive, machine-learning algorithms to analyze the microbial communities in coral mucus or tissue and identify microbial predictors of SCTLD, similar to work that identified microbial predictors of environmental features within reef seawater microbiomes (Glasl *et al.*, 2019). This could allow scientists the potential to identify corals afflicted with SCTLD before entire colonies are killed, and within the timeline of fieldwork or research cruises. Additionally, as more is learned about the identity of individual marine pathogens, then targeted pathogen identification approaches in novel systems may become more straightforward.

3.4. Conclusion

Stony Coral Tissue Loss Disease has collectively affected hundreds of kilometers of coastal and offshore reefs in the Caribbean, with no present indication of stopping. This study developed and

implemented a field-based, rapid microbiome characterization pipeline in the USVI, an area more recently affected by the SCTLD outbreak. Following successful sequencing on the Illumina iSeq 100, we identified 25 SCTLD bioindicator ASVs that may represent putative pathogens, including, *V. harveyi*, a bacterium known to be pathogenic in other marine systems. Many of the 25 bioindicator ASV sequences enriched in diseased coral were recovered in near-coral seawater, a potential reservoir for pathogens and the hypothesized vector for SCTLD. Interestingly, four of the SCTLD bioindicator ASVs identified in our study exactly matched sequences previously reported as enriched in SCTLD lesion samples. Phylogenetic analysis revealed that many of the disease bioindicator ASVs were related to likely novel coral or coral-associated disease bacteria. Future investigations aimed at isolating and characterizing those microorganisms and other SCTLD bioindicator bacteria would better determine if these organisms are pathogens or opportunists, and how they potentially target and grow around or within coral hosts. In the present study, the successful integration of a rapid pipeline for studying coral disease generated data more quickly, and subsequent analysis revealed differences in microbiome structure associated with the SCTLD outbreak in the USVI. This contributes to the growing body of literature on SCTLD that is largely focused in Florida, USA. Finally, we found that this rapid microbiome characterization approach worked well for identifying microbial bioindicators of coral disease, and it may have useful applications to marine diseases more broadly.

4. EXPERIMENTAL PROCEDURES

4.1 Sample collection

Coral colonies showing active Stony Coral Tissue Loss Disease (SCTLD) and nearby completely healthy colonies were sampled on February 11 and 13, 2020 on Buck Island (18.27883°, –64.89833°), and Black Point (18.3445°, –64.98595°) reefs, respectively, in St. Thomas, USVI

(Fig. 1, Table 1). Buck Island was considered a recent outbreak site where disease first emerged in January 2020, whereas Black Point had SCTLD since at least January 2019. Coral species sampled were *Montastraea cavernosa* (Buck Island and Black Point; SW n = 20, Coral n = 18), *Colpophyllia natans* (Buck Island and Black Point, n = 16), *Meandrina meandrites* (Buck Island, n = 9), and *Orbicella franksi* (Buck Island, n = 6) (Table 1). SCTLD was identified by single or multi-focal lesions of bleached or necrotic tissue with epiphytic algae colonizing the recently dead and exposed skeleton (Fig. 2). At both reefs, some paling of colonies was apparent, especially on *Orbicella* spp., as a result of a recent bleaching event in October 2019. Due to this, it was challenging to distinguish SCTLD from white plague-type diseases, which generally occur following bleaching events (Miller *et al.*, 2009). As a result, we avoided sampling *Orbicella* spp., except when it was clear the colony had regained full coloration and the disease lesion was consistent with SCTLD infection.

To investigate if putative pathogens were recoverable from seawater surrounding diseased colonies, near-coral seawater was sampled 2-5 cm away from each coral colony prior to tissue sampling via negative pressure with a 60 ml Luer-lock syringe (BD, Franklin Lakes, NJ, USA). Two seawater samples were collected over each colony displaying SCTLD lesions: one sample was taken directly above healthy tissue approximately 10 cm away from the lesion, when possible, and a second sample over diseased tissue. Syringes were placed in a dive collection bag for the duration of the dive. Once on board the boat, the seawater was filtered through a 0.22 μm filter (25 mm, Supor, Pall, Port Washington, NY, USA) and the filter with holder was placed in a Whirl-pak bag and kept on ice until returning to the shore. While on shore, filters were placed in sterile 2 ml cryovials (Simport, Beloeil, QC, Canada) and frozen in a liquid nitrogen dry shipper.

After near-coral seawater sampling, samples of tissue and mucus mixed together (referred to as coral samples) were collected. One sample was collected from each healthy colony and two from each diseased colony. For the two samples collected from each diseased colony, one was collected from the interface between healthy and newly bleached tissue (Fig. 2), and the other from healthy tissue approximately 10 cm away from the disease interface. When limited healthy tissue remained on a diseased colony, the coral sample was collected approximately 3 to 5 cm away from the disease lesion interface. The coral samples were collected with 10 ml non-Luer lock syringes (BD) by agitating and disrupting a small area of the tissue surface with the syringe tip while simultaneously aspirating the resulting suspended tissue and mucus into the syringe. To control for the significant amount of seawater and seawater-associated microbiota unavoidably captured during the collection of the coral samples, a total of nine 10 ml syringes of ambient reef seawater were collected from approximately 1 m off the reef benthos, (hereafter referred to as "Syringe Method Control" samples). Immediately after collection, the syringes were placed in a Whirl-pak bag to prevent the loss of sample while underwater. Once back on board the boat, samples were transferred to 15 ml sterile conical tubes and placed in a 4°C cooler. Upon returning to the laboratory, samples were frozen to –20°C until analysis.

The physical and chemical environment of the surrounding seawater was characterized by measuring temperature, salinity, dissolved oxygen, pH, and turbidity using an Exo2 multiparameter sonde (YSI, Yellow Springs, OH, USA) (Table S1). The sonde probes were calibrated following manufacturer's protocols on the day before sampling (February 10, 2020).

4.2 DNA extraction, PCR, and sequencing

Protocols for preparing samples for sequencing were specifically designed for the Illumina iSeq 100 System (Illumina Inc., San Diego, CA, USA), a portable, high-quality sequencing

technology. In an approximately 1 cu. ft. size, the Illumina iSeq 100 System produces 4 million paired-end 150 bp sequence reads of high quality (<1% error rate) that can be offloaded and processed on a standard laptop without the need for Wi-Fi, making it an attractive technology to adapt for field-based microbiome studies. We brought the iSeq 100 System to a home rental in the USVI, which we transformed into a remote laboratory where we successfully conducted all DNA extractions, Polymerase Chain Reaction (PCR) and subsequent sequencing.

DNA was extracted from seawater, coral, and syringe method control samples, along with associated extraction controls, using the DNeasy PowerBiofilm Kit (Qiagen, Germantown, MD, USA). Modifications at the beginning of the extraction protocol were applied based on the sample type. For filtered seawater samples, the 0.22 μm filter was placed directly into the bead tube, and then manufacturer instructions were followed. For coral and syringe method control samples, samples were thawed at room temperature, then immediately transferred to 4°C prior to extraction. Samples then were vortexed for 10 seconds and 1.8 ml of each sample was transferred to a bead tube. Samples were centrifuged at 12,045 rcf (maximum rcf available on centrifuge) for 10 min to concentrate tissue, mucus, and the associated microorganisms at the bottom of the tube, and supernatant was removed. For samples that were very clear (very little tissue collected via syringe) and for syringe method control samples, a second aliquot of 1.8 ml of sample was centrifuged on top of the existing pellet to capture more microorganisms. The extraction proceeded by following the manufacturer's protocol. Six DNA extraction controls, three for each sample type, were generated by following the manufacturer's protocol using: blank bead tubes for coral and syringe method control samples (named D1-D3) and unused 0.22 μm filters placed in bead tubes for seawater samples (named D4-D6).

A two-stage PCR process was used to prepare the samples for sequencing. In the first stage, PCR was used to amplify the V4 region of the small sub-unit ribosomal RNA (SSU rRNA) gene of bacteria and archaea. The amount of DNA added and the total reaction volume of this first PCR varied by sample type. For each PCR, 2 µl of coral and syringe method control template DNA was added to a final volume of 50 µl. 1 µl template in a 25 µl total reaction volume was used for seawater samples. For negative PCR controls, 1 or 2 µl of sterile PCR-grade water was used in 25 or 50 µl (total volume) reactions, respectively. One Human Microbiome Project mock community, Genomic DNA from Microbial Mock Community B (even, low concentration), v5.1L, for 16S rRNA Gene Sequencing, HM-782D was included as a sequencing control using 1 µl DNA in a 25 µl reaction. 50 µl reactions contained 0.5 µl polymerase (GoTaq, Promega, Madison, WI, USA), 1 µl each of 10 µM forward and reverse primers, 1 µl of 10 mM dNTPs (Promega), 5 µl $MgCl_2$ (GoTaq), 10 µl 5X colorless flexi buffer (GoTaq), and 29.5 µl UV-sterilized, PCR-grade water. 25 µl reactions used the same proportions of reagents as 50 µl reactions. Earth microbiome project primers revised for marine microbiomes, 515F and 806R, targeted bacteria and archaea and were used with Illumina-specific adapters (Apprill *et al.*, 2015; Parada *et al.*, 2016). Two small, portable thermocyclers were used for the PCRs: the mini8 (miniPCR, Cambridge, MA, USA), which contained 8 wells and connected to a laptop for programming and initiation of the run, and the BentoLab (Bento Bioworks Ltd, London, UK), which contained 32 wells and was programmable as a unit. Using both machines was ideal because our targeted number of samples per iSeq 100 sequencing run was 40. The thermocycler program for the first stage PCR was: 2 min at 95°C, 35 cycles (coral and syringe method control) or 28 cycles (seawater) of 20 sec at 95°C, 20 sec at 55°C, and 5 min at 72°C, followed by 10 min at 72°C and a final hold at 12°C. The final hold at 12°C was used

558 due to the limitations of the BentoLab termocycler; samples were removed within an hour of the
559 completed PCR program and stored at 4°C until purification. The resulting PCR products from
560 coral and syringe method control samples were purified as follows: 30 µl of PCR product per
561 sample was mixed with 6 µl 5X loading dye (Bioline, London, UK) and separated using a 1.5%
562 agarose gel stained with SYBR Safe DNA gel stain (Invitrogen, Thermo Fisher Scientific,
563 Waltham, MA, USA). Bands of approximately 350 bp were excised by comparing to a 50 bp
564 ladder (Bioline), and subsequently purified using the MinElute Gel Extraction Kit (Qiagen)
565 following manufacturer protocols. For seawater PCR products, 5 µl of product mixed with 1 µl
566 5X loading dye was visualized on a 1% agarose gel to verify successful amplification, and the
567 remaining PCR product was purified with the MinElute PCR Purification Kit (Qiagen).
568 The second stage PCR procedure attached unique index primers to each sample using the
569 Nextera XT v2 set A kit (Illumina). Purified DNA (5 µl) from stage one PCR products was
570 added to a 50 µl reaction with the following: 5 µl Nextera index primer 1, 5 µl Nextera index
571 primer 2, 5 µl $MgCl_2$ (GoTaq), 10 µl 5X colorless buffer (GoTaq), 0.5 µl Taq polymerase
572 (GoTaq), 1 µl of 10 mM dNTPs (Promega), and 18.5 µl UV-sterilized, PCR-grade water. The
573 PCR was run on the BentoLab or mini8 thermocyclers with the following program: 3 min at
574 95°C, 8 cycles of 30 sec at 95°C, 30 sec at 55°C, 30 sec at 72°C, followed by 5 min at 72°C and
575 a final hold at 12°C. A subset of PCR products were visualized on a 1% agarose gel stained with
576 SYBR Safe DNA gel stain (Invitrogen) using 5 µl product with 1 µl 5X loading dye (BioLine) to
577 verify bands of approximately 450 bp, indicating successful attachment of sample-specific
578 indexes. The stage two PCR products were purified with the MinElute PCR purification kit
579 (Qiagen) following manufacturer protocols. Purified products were quantified using the Qubit
580 2.0 fluorometer dsDNA high sensitivity (HS) assay (Invitrogen) following manufacturer

protocols to obtain stock concentrations in ng/µl. Concentrations were then converted to nM assuming average amplicon length of 450 bp and average nucleotide mass of 660 g/mol. Samples were diluted to 5 nM and pooled. Pooled samples were quantified via Qubit HS assay as before, and diluted to 1 nM, quantified again, and diluted to a loading concentration of 90 pM. A 10% spike-in of 90 pM PhiX Control v3 (Illumina, Inc.) was added to the pooled 90 pM library and 20 µl of the resulting library was run on the iSeq 100 System using paired-end 150 bp sequencing with adapter removal. Samples were sequenced over three sequencing runs.

4.3 Data analysis

All R scripts used for generating ASVs and producing figures were uploaded to GitHub. Forward reads were exclusively used for the downstream processing and data analysis due to minimal overlap between forward and reverse reads. The DADA2 pipeline (v.1.17.3; with parameters: *filterAndTrim* function: trimLeft = 19, truncLen = 145, maxN = 0, maxEE = 1, rm.phix = TRUE, compress = TRUE, multithread = TRUE) was used to remove the 515F and 806R primers from all sequence reads, filter the reads for quality and chimeras, and generate amplicon sequence variants (ASVs) for each sample (Callahan *et al.*, 2016). This resulted in 17,190 ASVs of the same length (126 bp) across all samples. Taxonomy was assigned using the SILVA SSU rRNA database down to the species level where applicable (v.132) (Quast *et al.*, 2012). ASVs that classified to mitochondria, chloroplast, eukaryote, or an unknown Kingdom were removed from the analysis, resulting in 7,366 remaining ASVs. We further filtered our dataset to remove possible contaminants introduced by DNA extraction reagents and introduced by seawater into coral samples. The R package *decontam* (v. 1.6.0) was used to identify and remove DNA extraction contaminants in all samples (seawater, coral, and syringe method control) by using a combined frequency and prevalence method employing default parameters (Davis *et al.*, 2018).

The method identified 26 ASV contaminants, of which only 11 contained enriched frequency in DNA extraction controls so those 11 ASVs were removed (DNA extraction contaminants summarized in Appendix 1). Because the syringe method by nature collects a significant portion of seawater, the coral samples were, in essence, "contaminated" by seawater and thus, the microorganisms most likely derived from seawater rather than coral tissue were removed. To do this, the coral samples were compared with the nine syringe method controls (seawater collected approximately a meter off of the benthos) using the prevalence model in *decontam,* which compares the presence/absence of ASVs within the syringe method controls to the coral samples. After applying the prevalence method, analysis of the distribution of the decontam score, *P*, was conducted to determine an appropriate threshold for identifying whether an ASV was a "contaminant" (i.e. seawater-derived) or an ASV that was tissue-associated. A threshold of 0.1 was chosen in order to be most conservative. While this conservative approach did not remove all ASVs typical of oligotrophic seawater taxa (e.g. *Synechococcus, Prochlorococcus*), a conservative approach here was necessary given the study goals of identifying potential SCTLD-associated ASVs residing in the surrounding seawater. The 184 ASVs identified as most prevalent in the nine syringe method controls (typically oligotrophic bacteria such as SAR11, *Prochlorococcus*, OM60 clade, *Synechococcus*, "*Candidatus* Actinomarina", AEGEAN-169 clade, etc.) were generally found at low relative abundance in the coral samples (max relative abundance = 0.0074%) and were removed from the coral sample ASV table (contaminants summarized in Appendix 2). After the ASVs identified as contaminants were removed, the coral samples and the near-coral seawater samples were re-merged into one large dataset. The re-merged dataset then was filtered to remove sparse ASVs (present at a count of 0 in the majority

of samples) by removing ASVs with a count less than 0.5 when averaged across all samples. This left 2,010 ASVs, which were used for all downstream analyses.

Count data were transformed to relative abundance and coral microbial communities were visualized using stacked bar charts. Data were then further log transformed following the addition of a pseudo count of one in preparation for beta diversity analyses. Bray-Curtis dissimilarity between samples was calculated using the R package *vegan* (v.2.5.7) and the resulting dissimilarities were presented in a Principal Coordinates Analysis (PCoA) (Oksanen *et al.*, 2019). Permutational Analysis of Variance (PERMANOVA) with 999 permutations, using the *adonis* function in *vegan* (Oksanen *et al.*, 2019), compared the Bray-Curtis dissimilarity of healthy and diseased corals to test the hypothesis that coral microbiomes are significantly different between healthy and SCTLD-afflicted samples. PERMANOVA was also used to test the hypotheses that species, reef location, and health state nested within species significantly structure the coral microbial community. We tested the same hypotheses on the near-coral seawater directly overlying the coral colony to determine if species, reef location, or health drove microbiome community structure in near-coral seawater. Dispersion of beta diversity within coral samples was calculated by measuring the distance to centroid within the PCoA as grouped by health state (HH and HD compared to DD) by implementing the *betadisper* function in *vegan* (Oksanen *et al.*, 2019). Significant differences in dispersion by health state was determined by an independent Mann-Whitney U test. Additionally, variability of beta diversity was measured by extracting the Bray-Curtis dissimilarity values calculated within a coral condition (diseased or healthy).

To detect ASVs enriched in diseased coral compared to healthy coral, we employed the R package, *corncob* (v.0.1.0) (Martin *et al.*, 2020). ASV raw counts for each sample were input

into the corncob model, which models the relative abundances for each ASV with a logit-link for mean and dispersion. Differential abundance of each ASV was modeled as a linear function of health state. Health state was defined as either healthy (healthy tissue from either apparently healthy or diseased coral) or diseased (lesion from diseased coral). The hypotheses that the relative abundance of a given ASV changed significantly with respect to coral health state were tested with the parametric Wald test. The multiple comparisons were accounted for by using a Benjamini-Hochberg false discovery rate correction with a cutoff of 0.5. Each test was conducted on the set of coral samples from an individual coral, then results were compared across corals. Following analysis of significantly differentially abundant ASVs in corals, we hypothesized that disease-associated ASVs would be recoverable in the near-coral seawater and graphed relative abundances of each disease-associated ASV in the near-coral seawater. We then employed corncob to test each identified disease-associated ASV using the differential abundance method described above to see if it was enriched at significantly higher abundances in seawater over diseased coral compared to healthy coral or apparently healthy colonies. Disease-associated ASVs were considered SCTLD bioindicators if they were enriched in diseased coral. Further, we searched for exact sequence matches between the 126 bp sequences of disease-associated ASVs reported here to the same sequence region from existing SCTLD-associated ASVs of longer lengths (approx. 253 bp) reported in other studies that also used the DADA2 pipeline. This pipeline allowed for sequences to be reported along with each ASV, enabling cross-study comparison (Callahan *et al.*, 2017).

Sequences of SCTLD bioindicator ASVs, were identified to the species level, when possible, as part of the DADA2 pipeline. To obtain better genus and species-level identification of SCTLD bioindicator ASVs and to relate these ASVs to other studies of coral disease-

associated bacteria, we constructed phylogenetic trees for disease-associated ASVs classifying to *Vibrio, Arcobacter,* Rhizobiaceae, and Rhodobacteraceae. *Vibrio* and *Arcobacter* were targeted due to their increased representation in SCTLD-associated ASVs in this study and their previous association with SCTLD (Meyer *et al.*, 2019; sequences obtained from Table 1) and coral disease in general (Ben-Haim *et al.*, 2003; Ushijima *et al.*, 2012). Rhizobiaceae and Rhodobacteraceae were targeted for phylogenetic tree analysis given their previous association with SCTLD (Rosales *et al.*, 2020; sequences obtained from Supplementary Table S1). Phylogenetic trees of coral-associated *Vibrio* and Rhodobacteraceae bacteria previously constructed from the Coral Microbiome Database (Huggett and Apprill, 2019) were used as reference trees for the insertion of SCTLD-associated ASVs that classified as *Vibrio* or Rhodobacteraceae. Insertion of our short SCTLD-associated sequence reads was achieved using the 'quick add marked' tool in ARB (version 6.0.6.rev15220) (Ludwig, 2004). Trees produced from ARB were exported using xFig. Phylogenetic trees for *Arcobacter* and Rhizobiaceae were constructed de novo using tools from the CIPRES Science Gateway (Miller *et al.*, 2010). For each tree, long-read (~1,200 bp) 16S rRNA gene sequences from closely-related (>90% sequence similarity) culture collection type strains, strains isolated from the marine environment, or clone sequences from corals were recovered via BLAST searches of SCTLD-associated ASVs from the present study or previous studies (Meyer *et al.*, 2019; Rosales *et al.*, 2020) to the non-redundant nucleotide collection, compiled into a FASTA file, and used for a sequence alignment in MAFFT (v7.402) (Katoh, 2002). This sequence alignment was then used to generate a reference tree using RAxML-HPC (v.8) (Stamatakis, 2014) with the following commands to produce a bootstrapped maximum-likelihood best tree: raxmlHPC-HYBRID -T 4 -f a -N autoMRE -n [output_name] -s [input_alignment] -m GTRGAMMA -p 12345 -x 12345. Next, SCTLD-associated short

sequence reads were compiled into a FASTA file and added to the long-read sequence alignment in MAFFT using the "--addfragments" parameter. The sequence alignment with both short and long reads and the reference tree were then used as inputs for the Evolutionary Placement Algorithm, implemented in RAxML (Berger *et al.*, 2011). RAxML was called as: raxmlHPC-PTHREADS -T 12 -f v -n [output_name] -s [long_and_short_read_alignment] -m GTRGAMMA -p 12345 -t [reference_tree]. The output tree including short read sequences (RAxML_labelledTree.[output_name]) was visualized and saved using the interactive tree of life (iTOL v5.6.3) (Letunic and Bork, 2016).

Acknowledgements

The authors would like to thank Lei Ma, Joseph Townsend, Kathryn Cobleigh, Sonora Meiling, and Kelsey Beavers for field assistance and Illumina Inc. for technical assistance. Additionally, we would like to thank Laura Weber for assistance with iSeq protocol development and field assistance. This work was funded by The Tiffany & Co. Foundation, NSF OCE-1928753, OCE-1928761 and OCE-1938147, the Rockefeller Philanthropy Advisors, Dalio Foundation, and other generous donors of the Oceans 5 project. Samples were collected under permit DFW19057U. We would also like to thank Stefan Sievert, Harriet Alexander, and Tami Lieberman for helpful comments on the manuscript.

Conflict of Interest

The authors have no conflicts of interest to declare.

Data Accessibility

Raw sequence reads were deposited into the NCBI GenBank under BioProject accession number PRJNA672912. Metadata associated with the study are also found at BCO-DMO under dataset 833133 (https://www.bco-dmo.org/dataset/833133). All R scripts used to generate figures and

statistical tests are saved and publicly available on GitHub at https://github.com/CynthiaBecker/SCTLD-STT.

References

Aeby, G.S., Ushijima, B., Campbell, J.E., Jones, S., Williams, G.J., Meyer, J.L., et al. (2019) Pathogenesis of a tissue loss disease affecting multiple species of corals along the Florida Reef Tract. *Front Mar Sci* **6**: 678.

Apprill, A. (2019) On-site sequencing speeds up and re-directs field-based microbiology. *Env Microbiol Rep* **11**: 45–47.

Apprill, A., McNally, S., Parsons, R., and Weber, L. (2015) Minor revision to V4 region SSU rRNA 806R gene primer greatly increases detection of SAR11 bacterioplankton. *Aquat Microb Ecol* **75**: 129–137.

Ben-Haim, Y., Thompson, F.L., Thompson, C.C., Cnockaert, M.C., Hoste, B., Swings, J., and Rosenberg, E. (2003) *Vibrio coralliilyticus* sp. nov., a temperature-dependent pathogen of the coral *Pocillopora damicornis*. *Int J Syst Evol Micr* **53**: 309–315.

Berger, S.A., Krompass, D., and Stamatakis, A. (2011) Performance, Accuracy, and Web Server for Evolutionary Placement of Short Sequence Reads under Maximum Likelihood. *Systematic Biology* **60**: 291–302.

Burge, C.A., Kim, C.J.S., Lyles, J.M., and Harvell, C.D. (2013) Special Issue Oceans and Humans Health: The Ecology of Marine Opportunists. *Microb Ecol* **65**: 869–879.

Callahan, B.J., McMurdie, P.J., and Holmes, S.P. (2017) Exact sequence variants should replace operational taxonomic units in marker-gene data analysis. *ISME J* **11**: 2639–2643.

Callahan, B.J., McMurdie, P.J., Rosen, M.J., Han, A.W., Johnson, A.J.A., and Holmes, S.P. (2016) DADA2: High-resolution sample inference from Illumina amplicon data. *Nat Methods* **13**: 581–583.

Chen, Y.-H., Yang, S.-H., Tandon, K., Lu, C.-Y., Chen, H.-J., Shih, C.-J., and Tang, S.-L. (2019) A genomic view of coral-associated *Prosthecochloris* and a companion sulfate-reducing bacterium, bioRxiv.

Davis, N.M., Proctor, D.M., Holmes, S.P., Relman, D.A., and Callahan, B.J. (2018) Simple statistical identification and removal of contaminant sequences in marker-gene and metagenomics data. *Microbiome* **6**: 226.

Dobbelaere, T., Muller, E.M., Gramer, L.J., Holstein, D.M., and Hanert, E. (2020) Coupled Epidemio-Hydrodynamic Modeling to Understand the Spread of a Deadly Coral Disease in Florida. *Front Mar Sci* **7**: 591881.

Egan, S. and Gardiner, M. (2016) Microbial Dysbiosis: Rethinking Disease in Marine Ecosystems. *Front Microbiol* **7**:.

Florida Keys National Marine Sanctuary (2018) Case Definition: Stony Coral Tissue Loss Disease (SCTLD).

Glasl, B., Bourne, D.G., Frade, P.R., Thomas, T., Schaffelke, B., and Webster, N.S. (2019) Microbial indicators of environmental perturbations in coral reef ecosystems. *Microbiome* **7**: 94.

Grimes, D.J., Stemmler, J., Hada, H., May, E.B., Maneval, D., Hetrick, F.M., et al. (1984) *vibrio* species associated with mortality of sharks held in captivity. *Microbial Ecology* **10**: 271–282.

761 Huggett, M.J. and Apprill, A. (2019) Coral microbiome database: Integration of sequences
762 reveals high diversity and relatedness of coral-associated microbes. *Env Microbiol Rep*
763 **11**: 372–385.
764 Illumina, Inc. (2020) iSeq 100 Sequencing System Specification Sheet.
765 Katoh, K. (2002) MAFFT: a novel method for rapid multiple sequence alignment based on fast
766 Fourier transform. *Nucleic Acids Res* **30**: 3059–3066.
767 Kramer, P.R., Roth, L., and Lang, J. (2021) Map of Stony Coral Tissue Loss Disease Outbreak in
768 the Caribbean. *AGRRA*.
769 Letunic, I. and Bork, P. (2016) Interactive tree of life (iTOL) v3: an online tool for the display
770 and annotation of phylogenetic and other trees. *Nucleic Acids Res* **44**: W242–W245.
771 Liu, M., Huang, Z., Zhao, Q., and Shao, Z. (2019) *Cohaesibacter intestini* sp. nov., isolated from
772 the intestine of abalone, *Haliotis discus hannai*. *Int J Syst Evol Microbiol* **69**: 3202–3206.
773 Liu, P.-Y., Wu, W.-K., Chen, C.-C., Panyod, S., Sheen, L.-Y., and Wu, M.-S. (2020) Evaluation
774 of Compatibility of 16S rRNA V3V4 and V4 Amplicon Libraries for Clinical
775 Microbiome Profiling, Microbiology.
776 Ludwig, W. (2004) ARB: a software environment for sequence data. *Nucleic Acids Res* **32**:
777 1363–1371.
778 Luna, G.M., Bongiorni, L., Gili, C., Biavasco, F., and Danovaro, R. (2010) *Vibrio harveyi* as a
779 causative agent of the White Syndrome in tropical stony corals. *Env Microbiol Rep* **2**:
780 120–127.
781 MacKnight, N.J., Cobleigh, K., Lasseigne, D., Chaves-Fonnegra, A., Gutting, A., Dimos, B., et
782 al. (2021) Microbial dysbiosis reflects disease resistance in diverse coral species.
783 *Commun Biol* **4**: 679.
784 Martin, B.D., Witten, D., and Willis, A.D. (2020) Modeling microbial abundances and dysbiosis
785 with beta-binomial regression. *Ann Appl Stat* **14**: 94–115.
786 Meiling, S., Muller, E.M., Smith, T.B., and Brandt, M.E. (2020) 3D Photogrammetry Reveals
787 Dynamics of Stony Coral Tissue Loss Disease (SCTLD) Lesion Progression Across a
788 Thermal Stress Event. *Front Mar Sci* **7**: 597643.
789 Mera, H. and Bourne, D.G. (2018) Disentangling causation: complex roles of coral-associated
790 microorganisms in disease: Disentangling coral disease causation. *Environ Microbiol* **20**:
791 431–449.
792 Meyer, J.L., Castellanos-Gell, J., Aeby, G.S., Häse, C.C., Ushijima, B., and Paul, V.J. (2019)
793 Microbial community shifts associated with the ongoing stony coral tissue loss disease
794 outbreak on the Florida Reef Tract. *Front Microbiol* **10**: 2244.
795 Miller, J., Muller, E., Rogers, C., Waara, R., Atkinson, A., Whelan, K.R.T., et al. (2009) Coral
796 disease following massive bleaching in 2005 causes 60% decline in coral cover on reefs
797 in the US Virgin Islands. *Coral Reefs* **28**: 925–937.
798 Miller, M.A., Pfeiffer, W., and Schwartz, T. (2010) Creating the cipres science gateway for
799 inference of large phylogenetic trees. 1–8.
800 Muller, E.M., Sartor, C., Alcaraz, N.I., and van Woesik, R. (2020) Spatial epidemiology of the
801 Stony-Coral-Tissue-Loss Disease in Florida. *Front Mar Sci* **7**: 163.
802 Neely, K.L., Macaulay, K.A., Hower, E.K., and Dobler, M.A. (2020) Effectiveness of topical
803 antibiotics in treating corals affected by Stony Coral Tissue Loss Disease. *PeerJ* **8**:
804 e9289.
805 Oksanen, J., Blanchet, F.G., Friendly, M., Kindt, R., Legendre, P., McGlinn, D., et al. (2019)
806 vegan: community ecology package. *R package version 25-4*.

807 Parada, A.E., Needham, D.M., and Fuhrman, J.A. (2016) Every base matters: assessing small
808 subunit rRNA primers for marine microbiomes with mock communities, time series and
809 global field samples. *Environ Microbiol* **18**: 1403–1414.
810 Pedersen, K., Verdonck, L., Austin, B., Austin, D.A., Blanch, A.R., Grimont, P.A.D., et al.
811 (1998) Taxonomic evidence that *Vibrio carchariae* Grimes et al, 1985 is a junior
812 synonym of *Vibrio harveyi* (Johnson and Shunk 1936) Baumann et al. 1981. *Int J Syst*
813 *Bacteriol* **48**: 749–758.
814 Precht, W.F., Gintert, B.E., Robbart, M.L., Fura, R., and van Woesik, R. (2016) Unprecedented
815 disease-related coral mortality in southeastern Florida. *Sci Rep* **6**: 31374.
816 Qu, L., Lai, Q., Zhu, F., Hong, X., Sun, X., and Shao, Z. (2011) *Cohaesibacter marisflavi* sp.
817 nov., isolated from sediment of a seawater pond used for sea cucumber culture, and
818 emended description of the genus *Cohaesibacter*. *Int J Syst Evol Microbiol* **61**: 762–766.
819 Quast, C., Pruesse, E., Yilmaz, P., Gerken, J., Schweer, T., Yarza, P., et al. (2012) The SILVA
820 ribosomal RNA gene database project: improved data processing and web-based tools.
821 *Nucleic Acids Res* **41**: D590–D596.
822 Rosales, S.M., Clark, A.S., Huebner, L.K., Ruzicka, R.R., and Muller, E.M. (2020)
823 *Rhodobacterales* and *Rhizobiales* are associated with stony coral tissue loss disease and
824 its suspected sources of transmission. *Front Microbiol* **11**: 681.
825 Silveira, C.B., Gregoracci, G.B., Coutinho, F.H., Silva, G.G.Z., Haggerty, J.M., de Oliveira,
826 L.S., et al. (2017) Bacterial community associated with the reef coral *Mussismilia*
827 *braziliensis's* momentum boundary layer over a diel cycle. *Front Microbiol* **8**: 784.
828 Soffer, N., Brandt, M.E., Correa, A.M., Smith, T.B., and Thurber, R.V. (2014) Potential role of
829 viruses in white plague coral disease. *ISME J* **8**: 271–283.
830 Stackebrandt, E. and Goebel, B.M. (1994) Taxonomic Note: A Place for DNA-DNA
831 Reassociation and 16S rRNA Sequence Analysis in the Present Species Definition in
832 Bacteriology. *International Journal of Systematic and Evolutionary Microbiology* **44**:
833 846–849.
834 Stamatakis, A. (2014) RAxML version 8: a tool for phylogenetic analysis and post-analysis of
835 large phylogenies. *Bioinformatics* **30**: 1312–1313.
836 Ushijima, B., Smith, A., Aeby, G.S., and Callahan, S.M. (2012) *vibrio owensii* induces the tissue
837 loss disease *Montipora* white syndrome in the Hawaiian reef coral *Montipora capitata*.
838 *PLoS ONE* **7**: e46717.
839 Vega Thurber, R., Mydlarz, L.D., Brandt, M., Harvell, D., Weil, E., Raymundo, L., et al. (2020)
840 Deciphering coral disease dynamics: Integrating host, microbiome, and the changing
841 environment. *Front Ecol Evol* **8**: 575927.
842 VI-CDAC (2021) Virgin Islands Coral Disease. *Stony Coral Tissue Loss Disease in the US*
843 *Virgin Islands*.
844 Viehman, S., Mills, D., Meichel, G., and Richardson, L. (2006) Culture and identification of
845 *Desulfovibrio* spp. from corals infected by black band disease on Dominican and Florida
846 Keys reefs. *Dis Aquat Org* **69**: 119–127.
847 Walton, C.J., Hayes, N.K., and Gilliam, D.S. (2018) Impacts of a regional, multi-year, multi-
848 species coral disease outbreak in southeast Florida. *Front Mar Sci* **5**: 323.
849 Wang, Q., Garrity, G.M., Tiedje, J.M., and Cole, J.R. (2007) Naïve Bayesian Classifier for Rapid
850 Assignment of rRNA Sequences into the New Bacterial Taxonomy. *AEM* **73**: 5261–5267.

851 Weber, L., Gonzalez-Díaz, P., Armenteros, M., and Apprill, A. (2019) The coral ecosphere: A
852 unique coral reef habitat that fosters coral-microbial interactions. *Limnol Oceanogr* **9999**:
853 1–16.
854

Figures

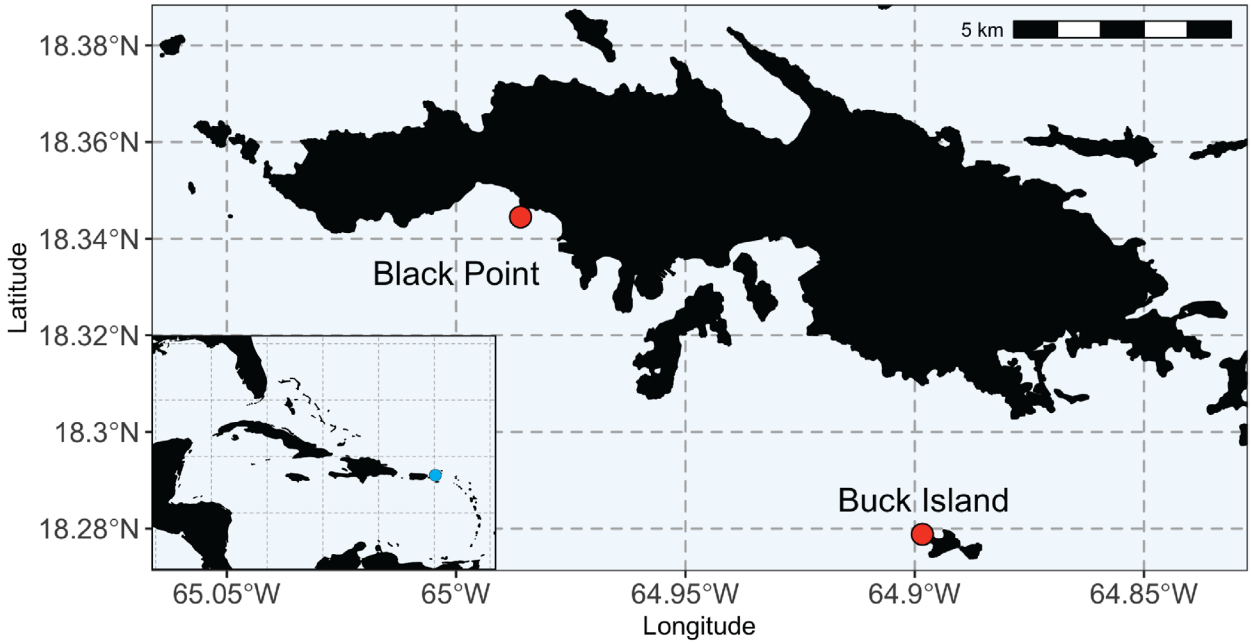

Fig. 1. Sampling locations at Black Point and Buck Island reefs in St. Thomas, U.S. Virgin Islands. St. Thomas sampling locations included a reef at Black Point, which was experiencing SCTLD for 13 months prior to sampling and a reef at Buck Island, in which SCTLD broke out in the month prior. Scale bar is 5 km with marks at every kilometer. Inset map shows the greater Caribbean with the blue dot noting the location of the U.S. Virgin Islands.

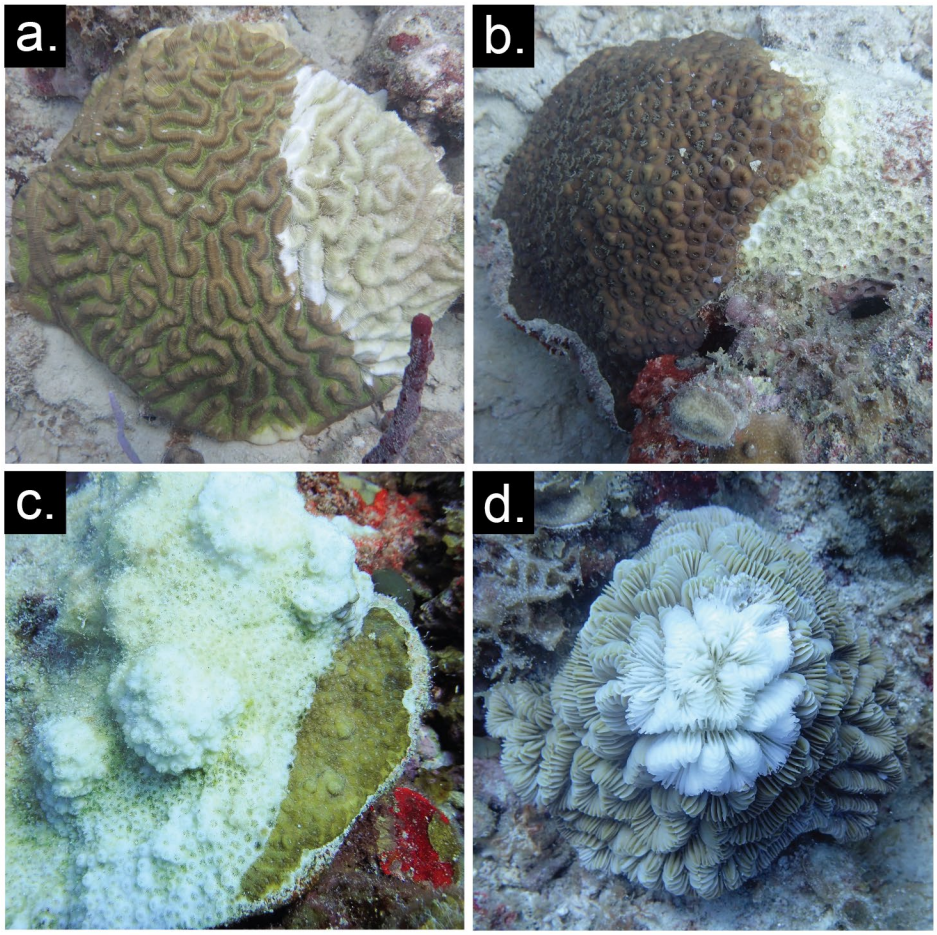

Fig. 2. Stony Coral Tissue Loss Disease lesions progress across healthy tissue. Photos represent typical disease appearance on the following corals included in the present study: (a) *Colpophyllia natans,* (b) *Montastraea cavernosa,* (c) *Orbicella franksi,* (d) *Meandrina meandrites*. Seawater and coral were sampled at the lesion front and 10 cm away from the lesion, or as far as possible from the lesion, when possible.

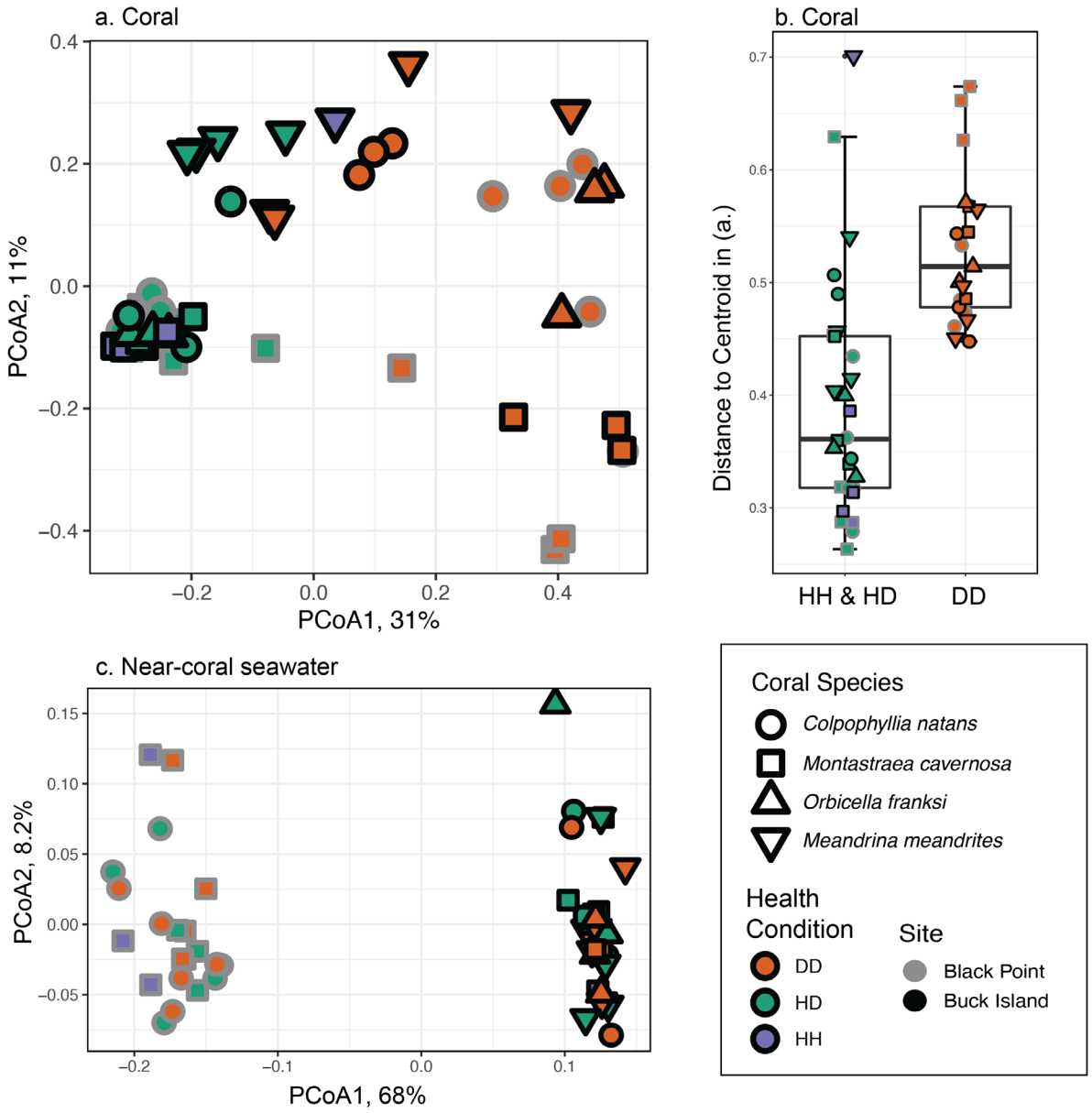

Fig. 3. Coral microbiomes differed according to health condition and near-coral seawater microbiomes differed according to site. (a) Principal coordinate analysis (PCoA) displays Bray-Curtis dissimilarity of coral microbial communities, (b) beta diversity dispersion of coral microbiomes represented by boxplots of the distance to centroid in (a), and (c) PCoA of Bray-Curtis dissimilarity in near-coral seawater microbiomes. Fill color represents health condition of the sample as diseased (DD, orange), healthy sample from a diseased colony (HD, green), or

healthy sample from an apparently healthy colony (HH, purple). Outline color indicates the reef where the sample was taken, which had either existing SCTLD infection (Black Point, gray), or was experiencing a recent (<1 month) outbreak of SCTLD (Buck Island, black). Shape represents species of coral sampled: *Colpophyllia natans* (circle), *Montastraea cavernosa* (square), *Orbicella franksi* (up triangle), and *Meandrina meandrites* (down triangle).

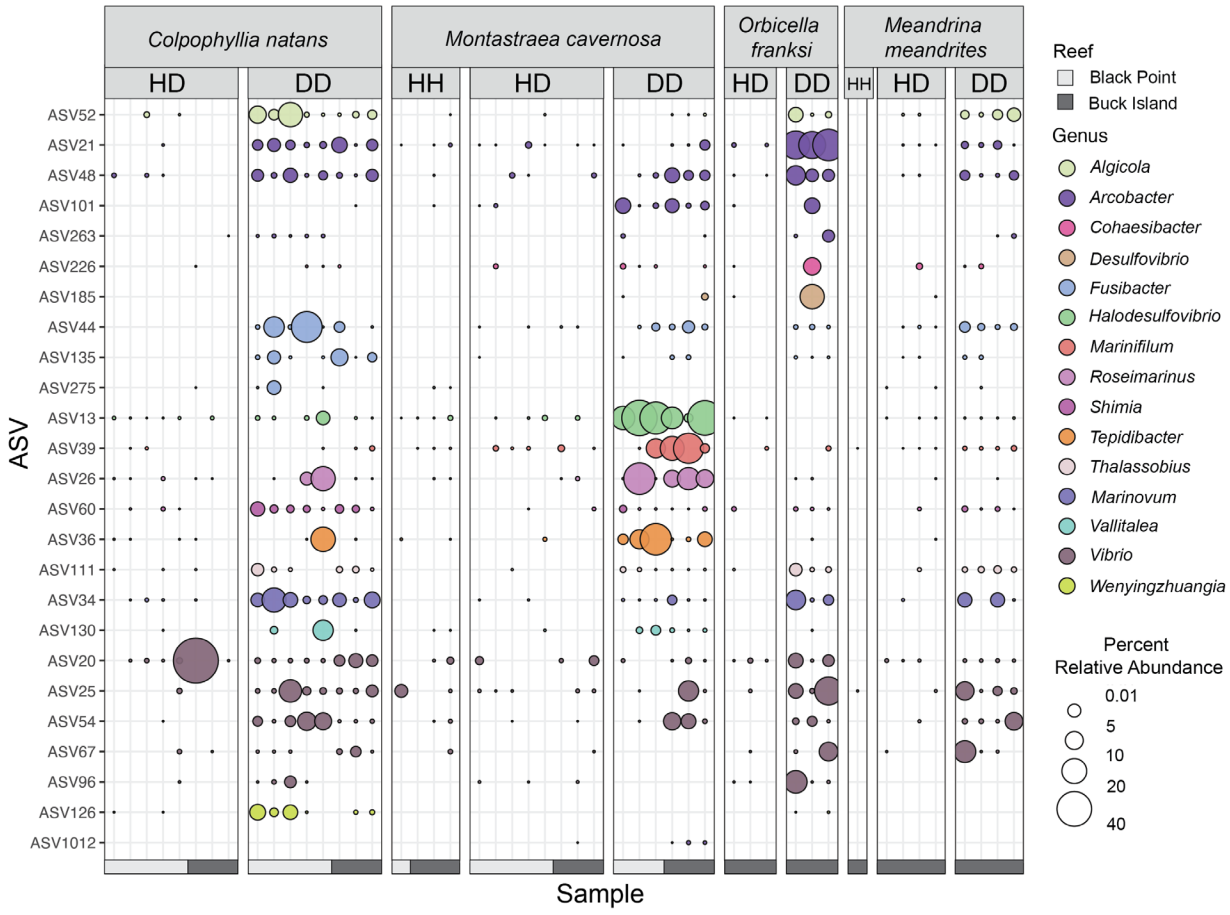

Fig. 4. Relative abundances of 25 SCTLD bioindicator ASVs significantly differentially enriched (FDR corrected p-value < 0.05) in diseased coral of at least one coral species. Samples on the x-axis are organized by coral species (*Colpophyllia natans*, *Montastraea cavernosa*, *Meandrina meandrites*, and *Orbicella franksi*), health state of the coral (healthy sample from apparently healthy colony = "HH", healthy sample from diseased colony = "HD", disease lesion = "DD"). Additionally, a color bar at the bottom indicates the coral was collected

at the Black Point (light gray) or at the Buck Island (dark gray). ASVs on the y-axis are organized and colored by Genus. Percent relative abundance of each ASV is represented by the size of the colored circle, with a percent relative abundance of zero represented by the absence of a circle or dot. The relative abundances were calculated after removing common seawater bacteria and archaea, which were determined using the syringe method control samples containing ambient reef seawater and with the R-package *decontam* (see methods).

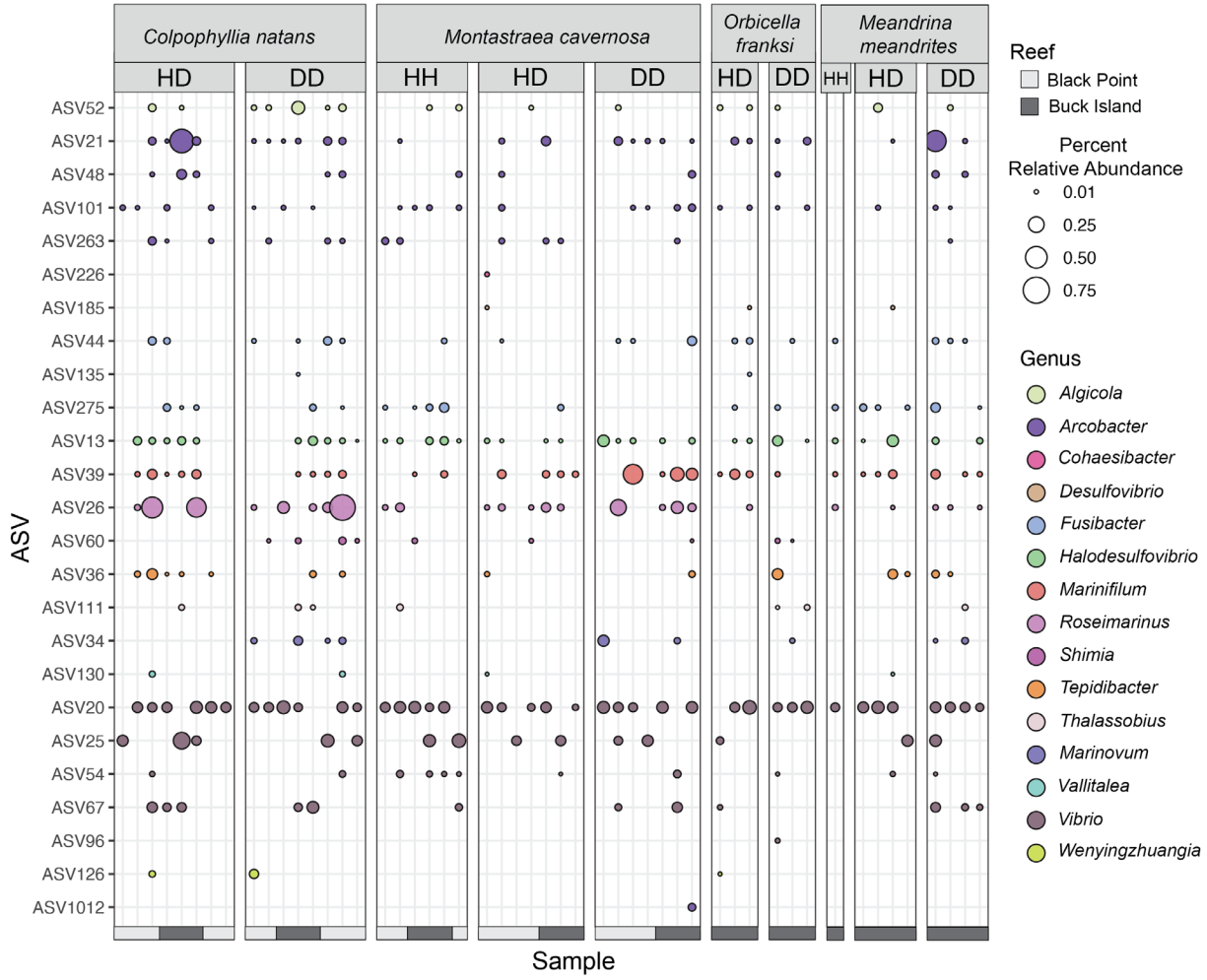

Fig. 5. SCTLD bioindicator ASVs identified in coral were found in near-coral seawater. Samples on the x-axis are organized by coral species (*Colpophyllia natans*, *Montastraea*

cavernosa, *Meandrina meandrites*, and *Orbicella franksi*), and health state of the coral (healthy sample from apparently healthy colony = "HH", healthy sample from diseased colony = "HD", disease lesion = "DD"). Additionally, a color bar at the bottom indicates whether the coral was collected at Black Point (light gray) or at Buck Island (dark gray). ASVs on the y-axis are organized and colored by Genus. Percent relative abundance of each ASV is represented by the size of the colored circle, with a percent relative abundance of zero represented by the absence of a circle or dot. ASVs graphed are those identified by differential abundance analysis as significantly enriched in diseased coral (FDR corrected p-value < 0.05) of at least one coral species.

Table 1. Number of near-coral seawater (SW) and coral samples collected from Buck Island or Black Point reefs on St. Thomas, USVI.

	Buck Island			Black Point		
	HH	HD	DD	HH	HD	DD
Colpophyllia natans	0	3	3	0	5	5
Montastraea cavernosa	3	3	3	3 SW* 1 Coral*	4 SW* 5 Coral*	4 SW* 3 Coral*
Orbicella franksi	0	3	3	0	0	0
Meandrina meandrites	1	4	4	0	0	0

*Sample sizes from *M. cavernosa* from the Existing disease reef were different between seawater and coral due to sampling and processing constraints**.**

Table 2. Bioindicator ASVs in the present study with 100% sequence similarity over 126 bp to SCTLD-associated ASVs of a longer length (~253 bp) identified by previous studies.

Family	Genus	ASV ID in present study	Enriched in diseased coral (Rosales et al. 2020)	Enriched in diseased coral (Meyer et al. 2019)

Pseudoalteromonadaceae	*Algicola*	52	no	**Yes**
Rhizobiaceae	*Cohaesibacter*	226	**Yes**	no
Rhodobacteraceae	*Thalassobius*	111	**Yes**	no
Vibrionaceae	*Vibrio*	54	no	**Yes**

922

923

Supplementary Figures and Tables

Table S1. Environmental conditions present at Buck Island or Black Point reefs

Reef	Buck Island	Black Point
Lat (dd)	18.27883	18.34450
Lon (dd)	–64.89833	–64.98595
Depth (m)	14.1	5.2
Temperature (°C)	26.88	26.98
Salinity	35.98	36.04
Dissolved Oxygen (% sat.)	102.5	105.0
pH	7.98	8.09
Turbidity (NTU)	–0.05	0.12

Table S2. Summary statistics of sequencing reads produced by three sequencing runs on the Illumina iSeq 100 System, outlined by sample type.

Sample Type	Average	Standard Deviation	Minimum	Maximum
Seawater (n = 51)	96,933	10,218	68,527	119,141
Coral (n = 49)	99,177	14,511	60,105	128,036
Syringe Method Control (n = 9)	96,290	7,542	85,728	113,293
DNA Extraction Control (n = 6)	19,418	11,672	1,908	34,118
PCR Negative Control (n = 3)	9,930	904	8,928	10,683
Mock Community (n = 3)	74,735	12,494	61,401	86,172

Table S3. Summary of coral species featuring significant enrichment (FDR corrected p-value < 0.05) of SCTLD bioindicator ASVs in disease lesion (DD) compared to healthy coral (HH and HD combined). White cells indicate no significant difference in the relative abundance of the ASV between healthy and diseased corals. Differential abundance of ASVs was calculated using the beta-binomial regression model of the R-package *corncob* and ASVs were considered significant at an FDR corrected p-value <0.05.

Family, Genus	ASV ID	*Colpophyllia natans*	*Montastraea cavernosa*	*Orbicella franksi*	*Meandrina meandrites*

Arcobacteraceae, *Arcobacter*	21				
Arcobacteraceae, *Arcobacter*	48				
Arcobacteraceae, *Arcobacter*	101				
Arcobacteraceae, *Arcobacter*	263				
Arcobacteraceae, *Arcobacter*	1012				
Desulfovibrionaceae, *Desulfovibrio*	185				
Desulfovibrionaceae, *Halodesulfovibrio*	13				
Family_XII, *Fusibacter*	44				
Family_XII, *Fusibacter*	135				
Family_XII, *Fusibacter*	275				
Flavobacteriaceae, *Wenyingzhuangia*	126				
Lachnospiraceae, *Vallitalea*	130				
Marinifilaceae, *Marinifilum*	39				
Peptostreptococcaceae, *Tepidibacter*	36				
Prolixibacteraceae, *Roseimarinus*	26				
Pseudoalteromonadacea, *Algicola*	52				
Rhizobiaceae, *Cohaesibacter*	226				
Rhodobacteraceae, *Shimia*	60				
Rhodobacteraceae, *Thalassobius*	111				
Rhodobacteraceae, unclassified	34				
Vibrionaceae, *Vibrio*	20				
Vibrionaceae, *Vibrio*	25				
Vibrionaceae, *Vibrio*	54				
Vibrionaceae, *Vibrio*	67				
Vibrionaceae, *Vibrio*	96				

937

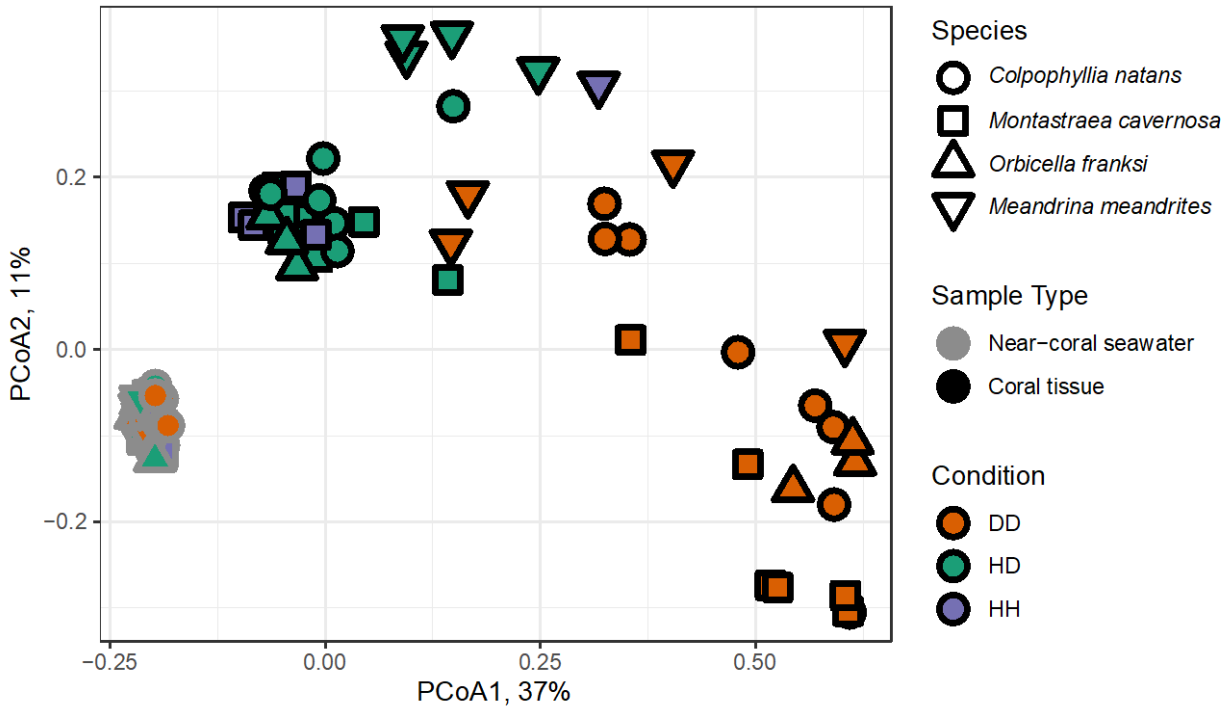

938

939 **Fig. S1. Principal coordinates analysis (PCoA) of Bray-Curtis dissimilarity between all**

940 **coral and seawater samples**. Seawater (gray outline) and coral (black outline) samples are

941 shaped by the coral species, *C. natans* (circle), *M. cavernosa* (square), *O. franksi* (up triangle),

942 and *M. meandrites* (down triangle). Colors indicate health condition where DD = SCTLD lesion

943 sample, HD = healthy sample on diseased colony, HH = healthy sample from apparently healthy

944 colony.

945

946

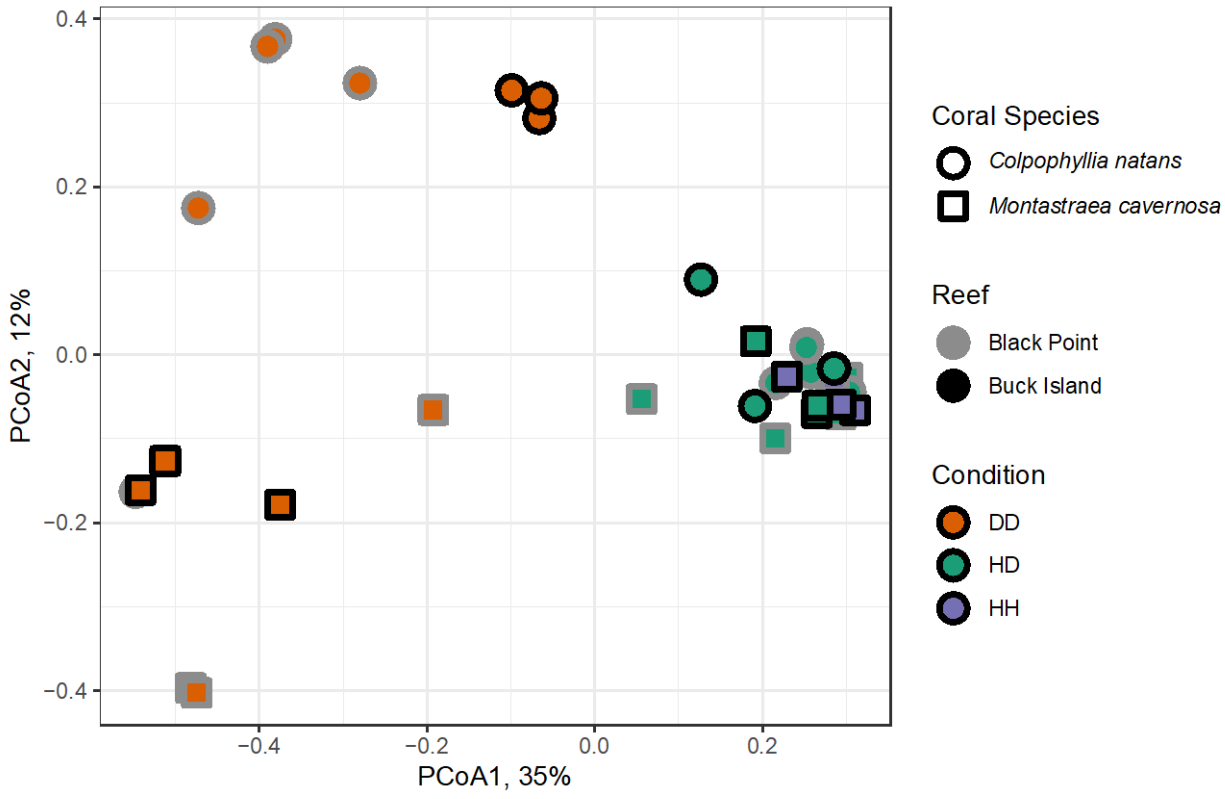

947

948 **Fig. S2. Principal coordinates analysis (PCoA) of Bray-Curtis dissimilarity between all**

949 **coral samples from *C. natans* and *M. cavernosa*.** Outline color denotes whether the corals

950 originated from the Black Point or Buck Island reef. Samples are shaped by the coral species, *C.*

951 *natans* (circle), *M. cavernosa* (square). Colors indicate health condition where DD = SCTLD

952 lesion sample, HD = healthy sample on diseased colony, HH = healthy sample from apparently

953 healthy colony.

954

955

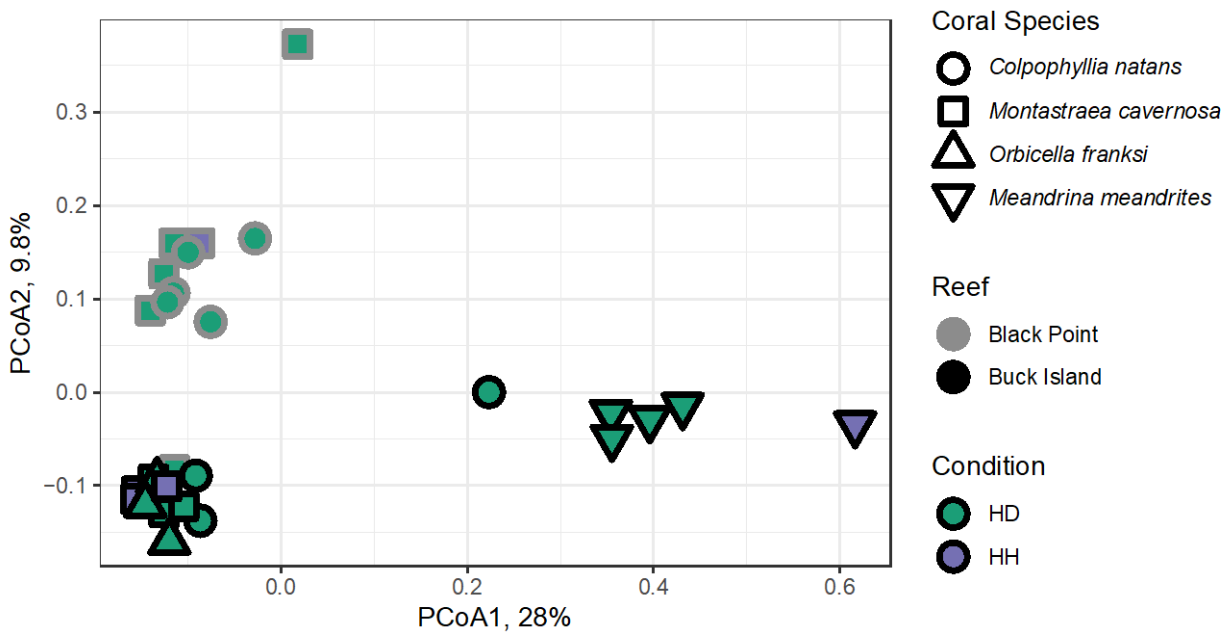

Fig. S3. **Principal coordinates analysis (PCoA) of Bray-Curtis dissimilarity within healthy coral samples only**. Outline color denotes whether the corals originated from the Black Point or Buck Island reef. Fill color represents whether the healthy sample was from a diseased colony (HD, green) or apparently healthy colony (HH, purple). Shape denotes the following coral species: *C. natans* (circle), *M. cavernosa* (square), *O. franksi* (up triangle), and *M. meandrites* (down triangle).

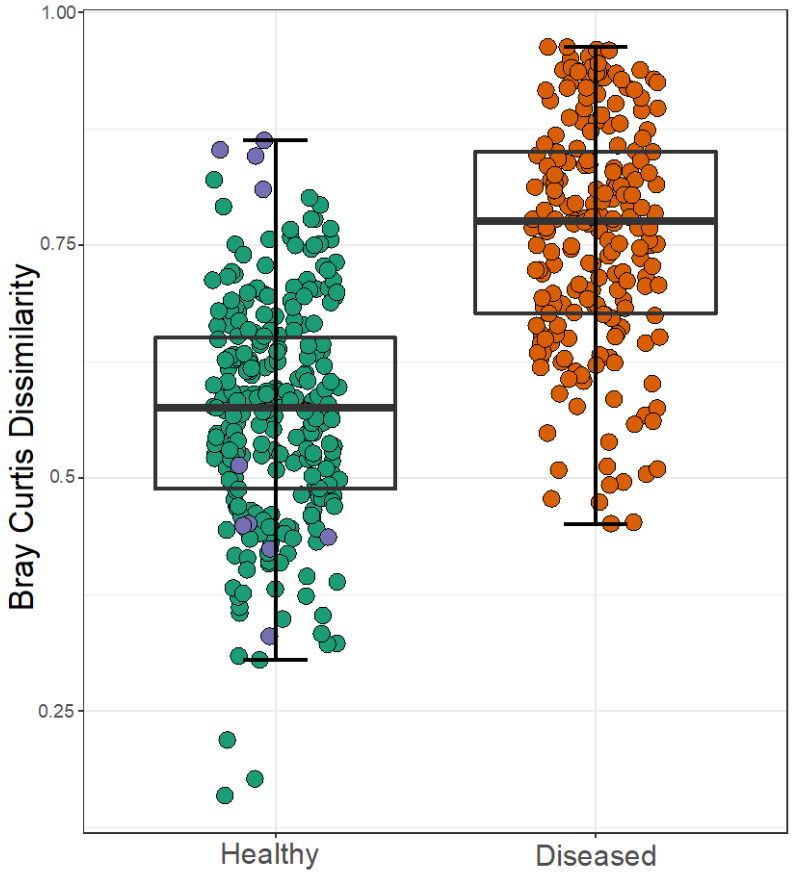

964

965 **Fig. S4**. **Boxplots denoting range in Bray-Curtis Dissimilarity values within healthy (HH =**

966 **purple and HD = green) and diseased (DD = orange) coral microbiomes**. Difference between

967 healthy and diseased Bray-Curtis dissimilarity values is significant by independent Mann-

968 Whitney U Test ($p < 0.001$).

969

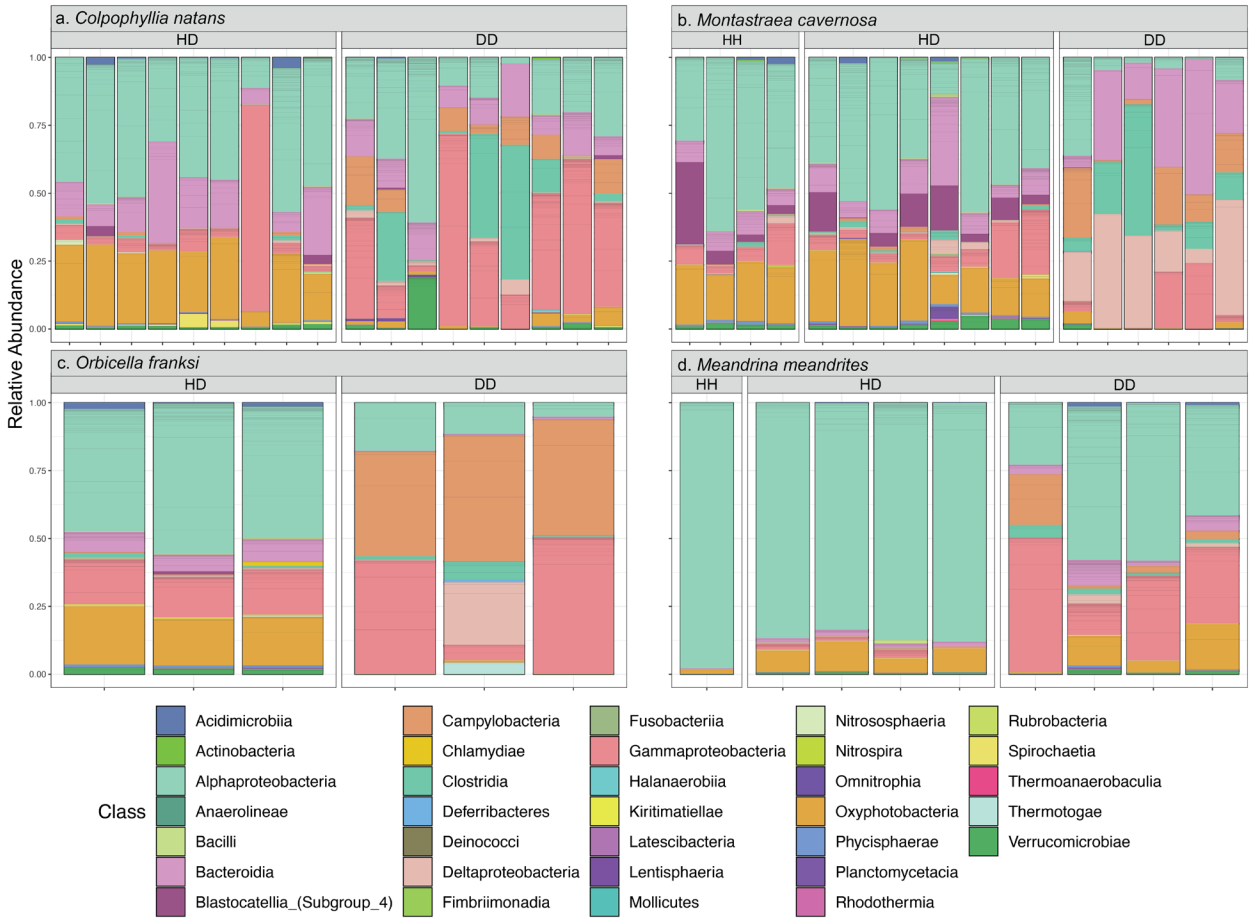

Fig. S5. Stacked bar chart of microbial relative abundances within corals in (a) *C. natans*, (b) *M. cavernosa*, (c) *O. franksi*, and (d) *M. meandrites*. Stacked bar charts are organized by coral health condition (HH = healthy sample from a healthy colony, HD = Apparently healthy sample from a diseased colony, DD = Disease lesion).

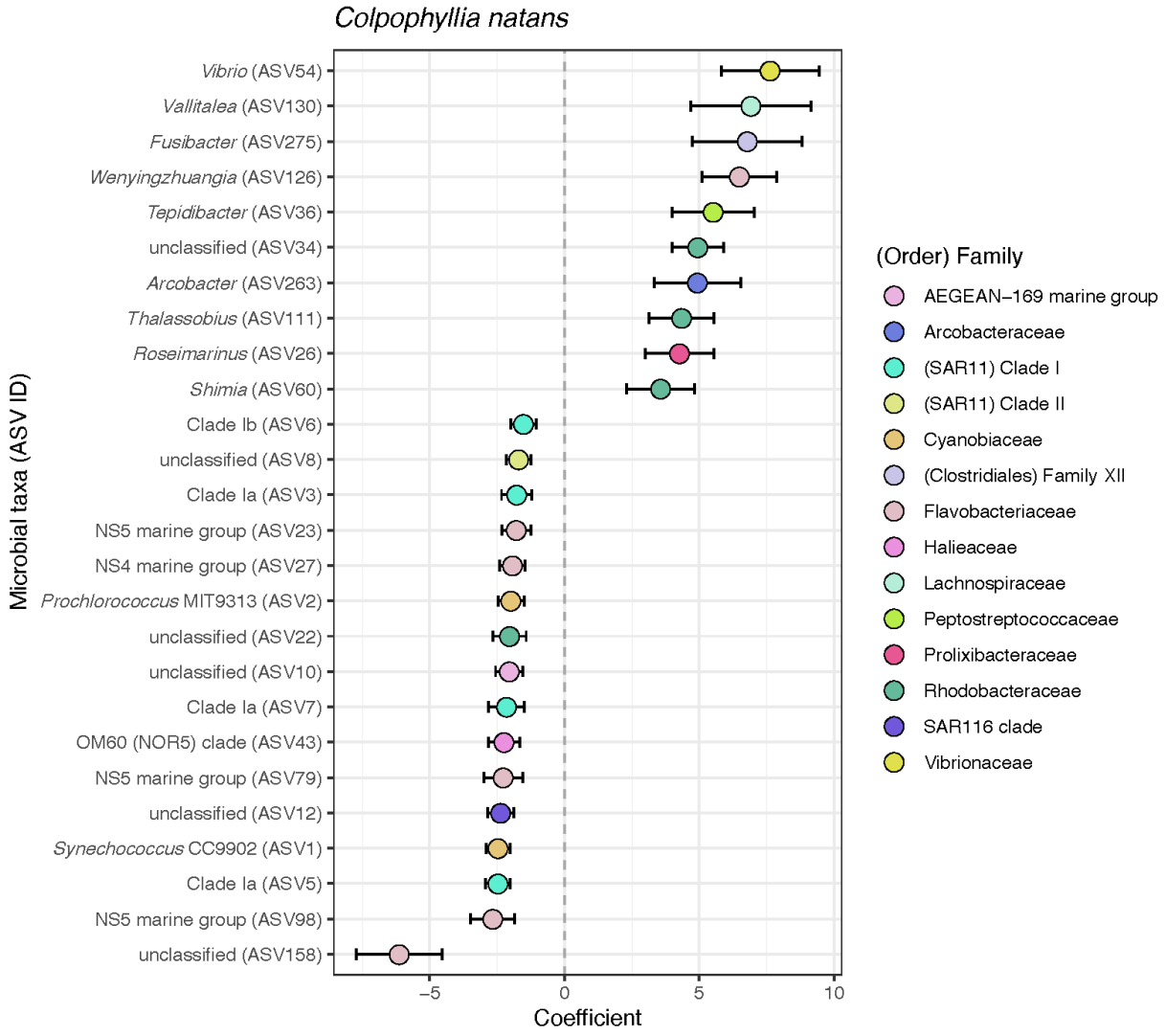

Fig. S6. Significantly differentially abundant ASVs between diseased and healthy coral in *Colpophyllia natans*. Positive coefficients indicate ASV relative abundance was enriched in diseased coral relative to healthy coral. Points are labeled by genera and ASV number, and colored by Family.

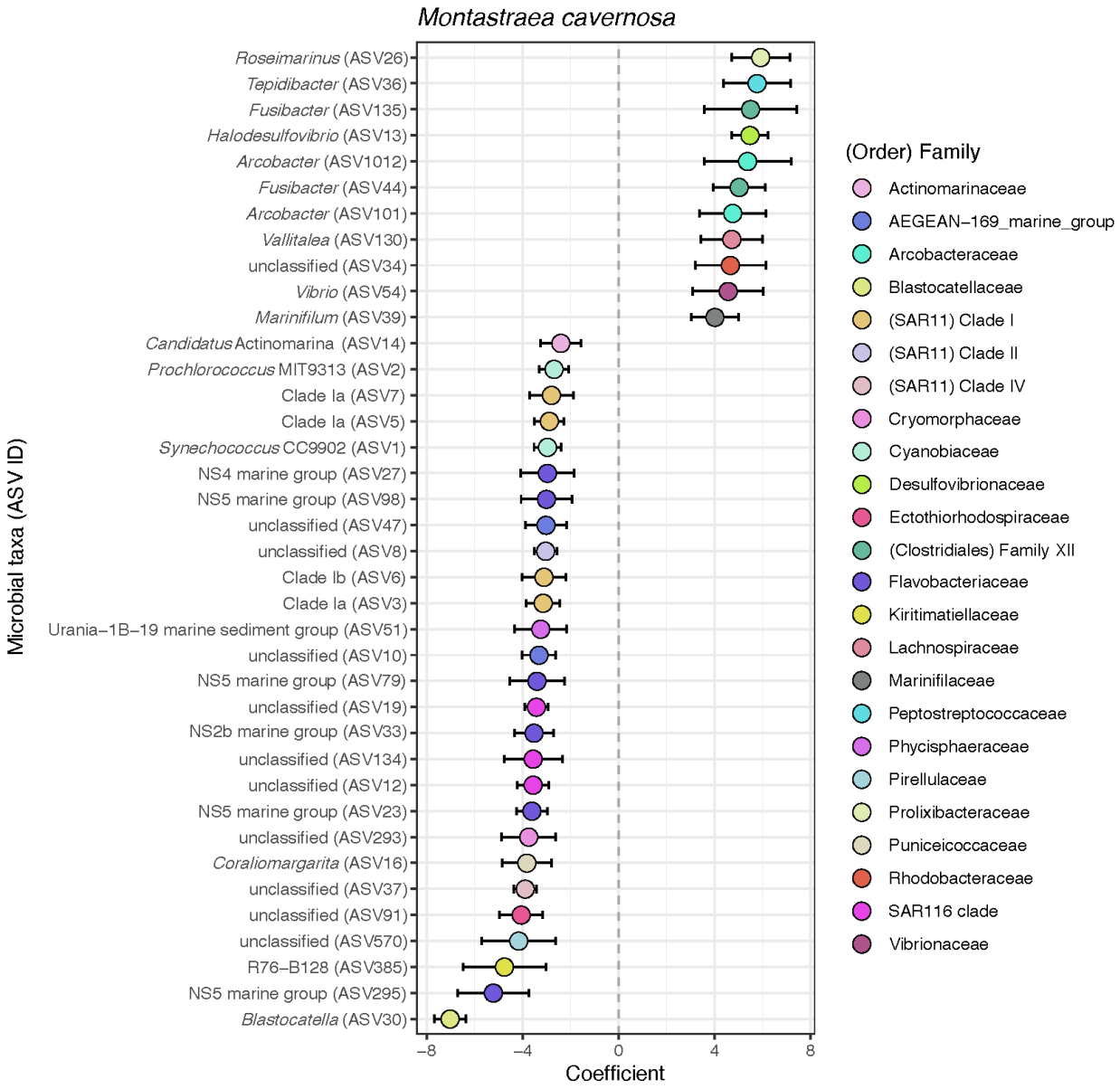

Fig. S7. Significantly differentially abundant ASVs between diseased and healthy coral in *Montastraea cavernosa*. Positive coefficients indicate ASV relative abundance was enriched in diseased relative to healthy coral. Points are labeled by genera and ASV number, and colored by Family.

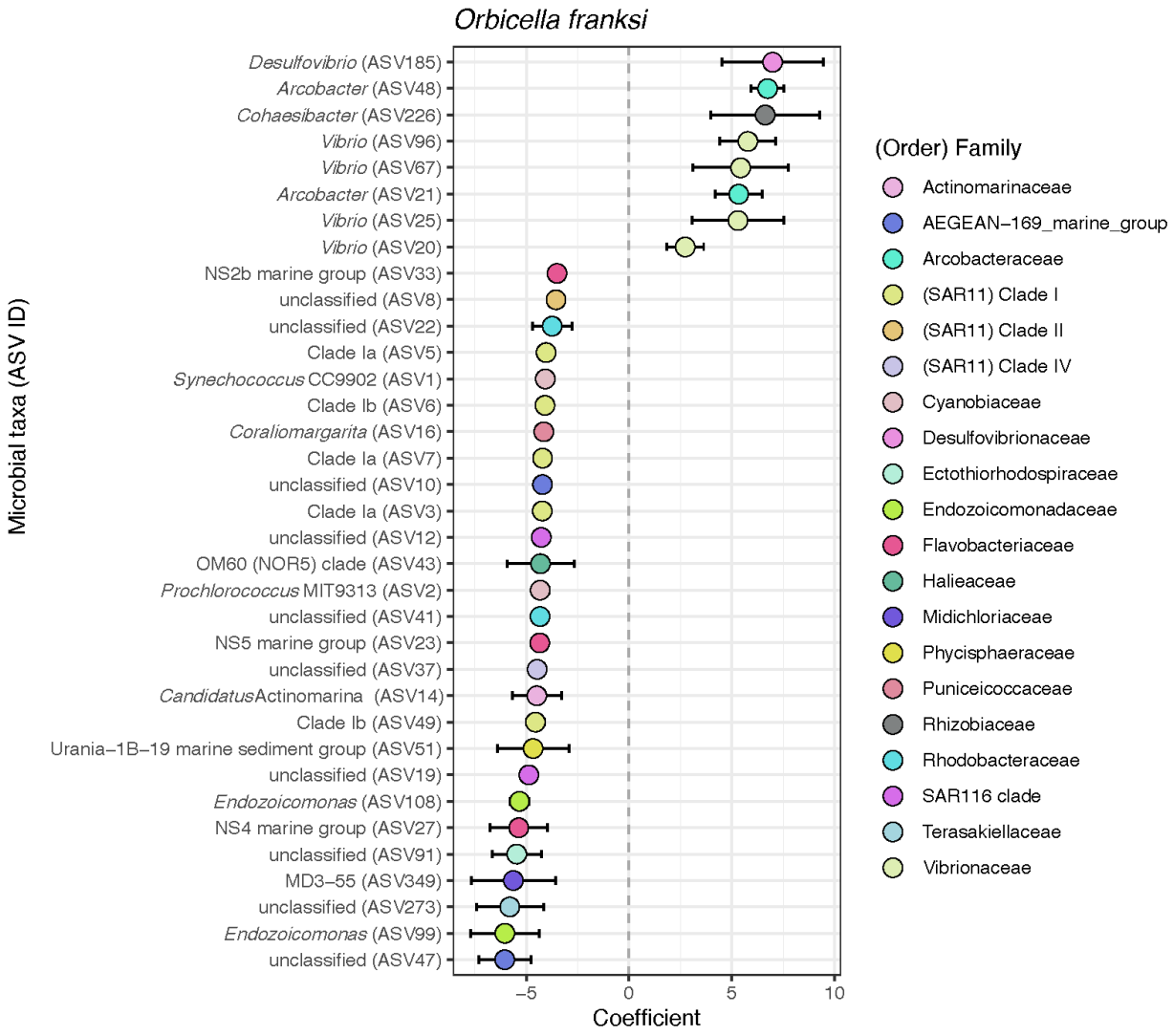

Fig. S8. Significantly differentially abundant ASVs between diseased and healthy coral in *Orbicella franksi*. Positive coefficients indicate ASV relative abundance was enriched in diseased relative to healthy coral. Points are labeled by genera and ASV number, and colored by Family.

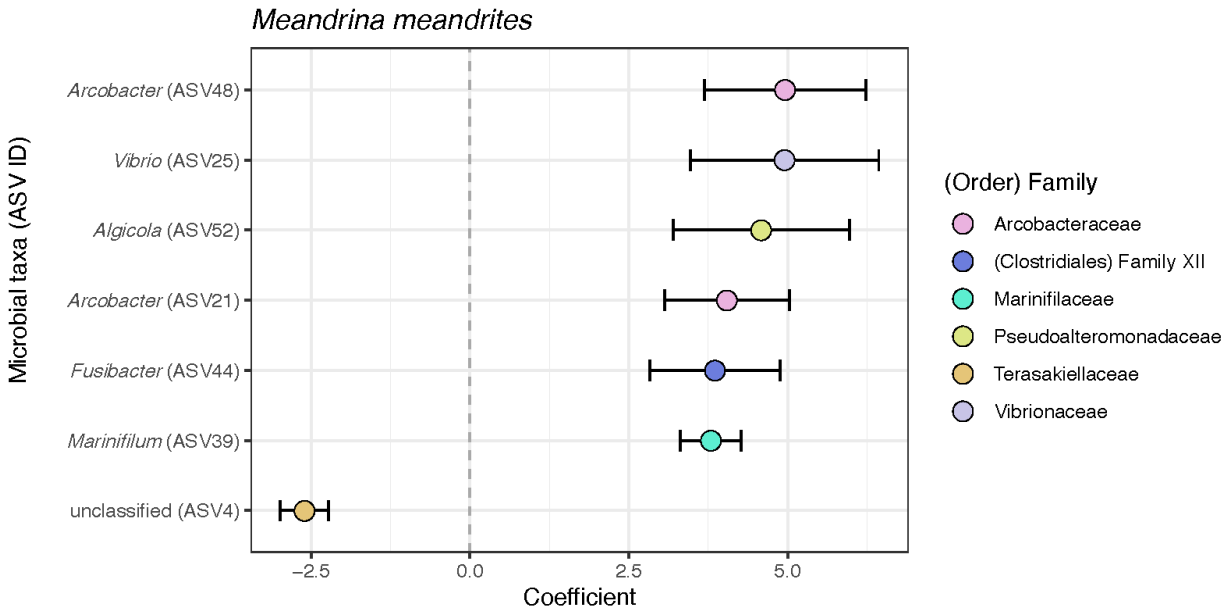

995

996 **Fig. S9. Significantly differentially abundant ASVs between diseased and healthy coral in**

997 ***Meandrina meandrites***. Positive coefficients indicate ASV relative abundance was enriched in

998 diseased relative to healthy coral. Points are labeled by genera and ASV number, and colored by

999 Family.

1000

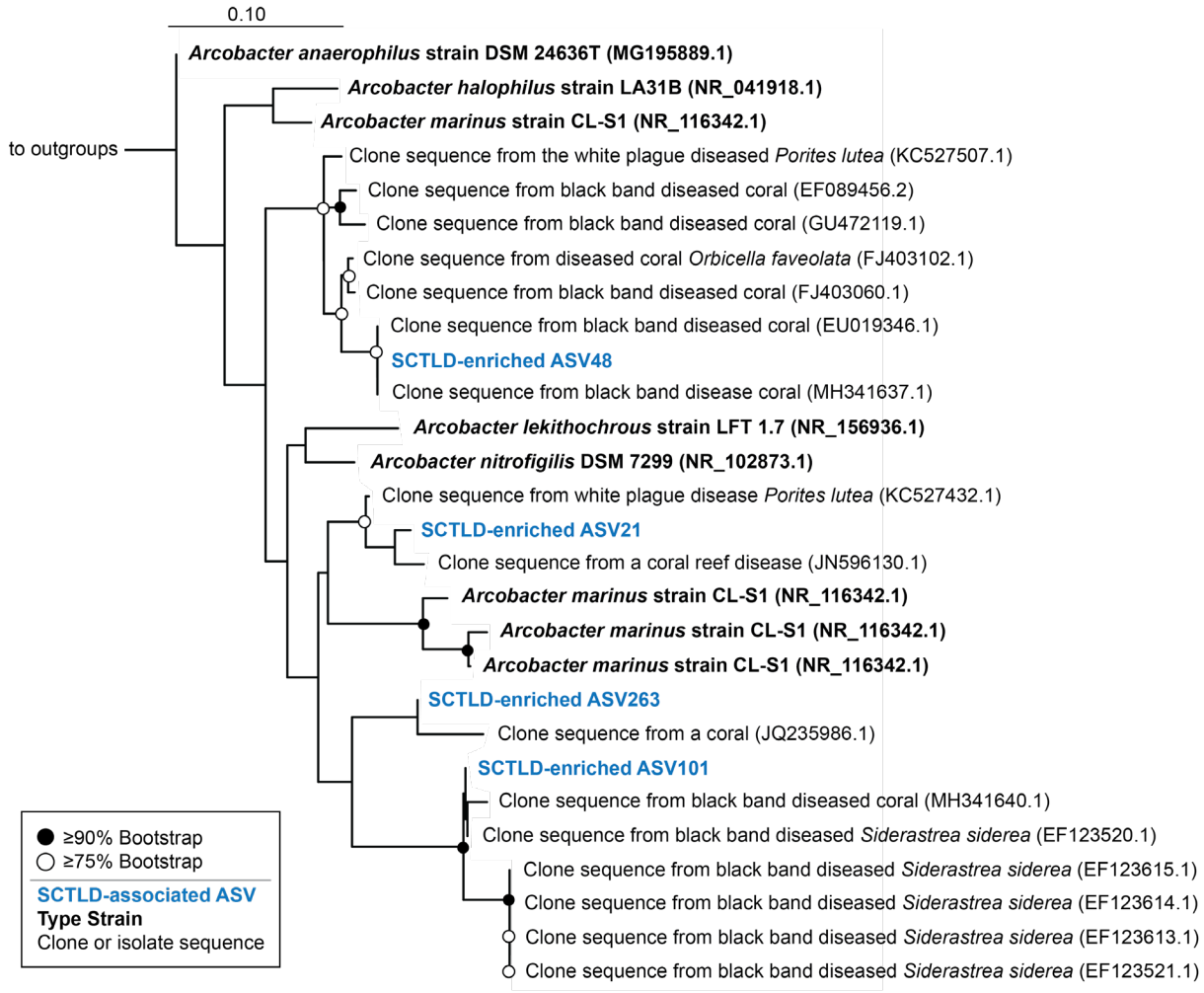

Fig. S10. Bioindicator ASVs from the genus *Arcobacter* closely related to isolates and clone sequences from diseased corals. Reference phylogenetic tree was produced using RAxML rapid bootstrapping with an automatic bootstrapping approach to produce the highest-scoring maximum likelihood tree using only longer-length sequences (black). SCTLD-associated ASVs (blue) identified by differential abundance analysis or by previous studies were added to the tree using the Evolutionary Placement Algorithm in RAxML. Colors represent qualitative information about the sequences as follows: Blue = SCTLD-associated ASVs from the present study, black bold = bacterial type strains, black = clone or bacterial isolate/strain sequences. GenBank accession numbers are located in parentheses following each taxa label. Circles at node

represent bootstrap values of ≥ 90% (filled-in circle) or ≥ 75% (empty circle). Bar indicates 10% sequence divergence. Tree was rooted using the 16S rRNA gene of *Streptococcus mutans* strain ATCC 25175 (NR_115733.1).

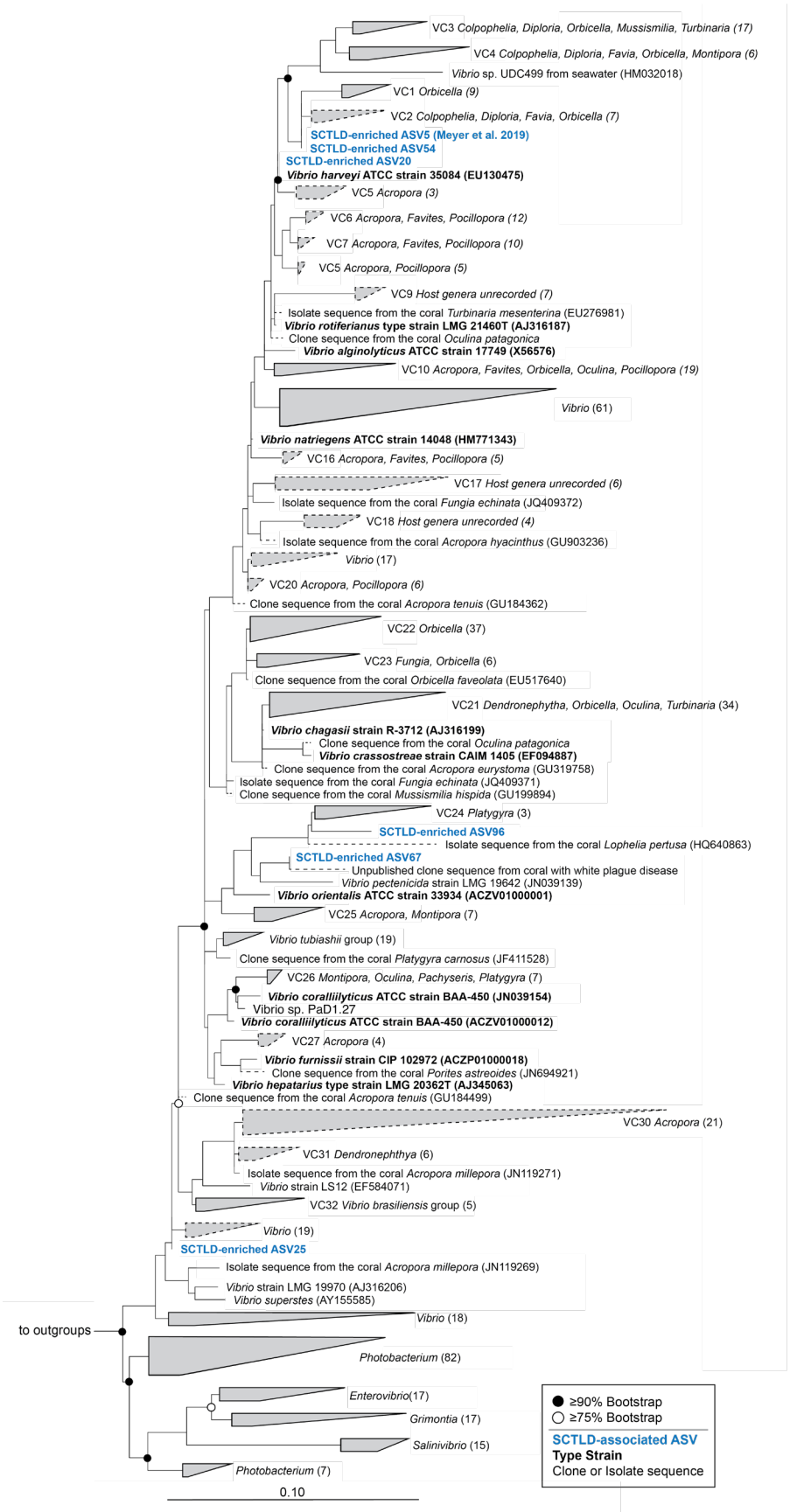
VC3 Colpophelia, Diploria, Orbicella, Mussismilia, Turbinaria (17)
VC4 Colpophelia, Diploria, Favia, Orbicella, Montipora (6)
Vibrio sp. UDC499 from seawater (HM032018)
VC1 Orbicella (9)
VC2 Colpophelia, Diploria, Favia, Orbicella (7)
SCTLD-enriched ASV5 (Meyer et al. 2019)
SCTLD-enriched ASV54
SCTLD-enriched ASV20
Vibrio harveyi ATCC strain 35084 (EU130475)
VC5 Acropora (3)
VC6 Acropora, Favites, Pocillopora (12)
VC7 Acropora, Favites, Pocillopora (10)
VC5 Acropora, Pocillopora (5)
VC9 Host genera unrecorded (7)
Isolate sequence from the coral Turbinaria mesenterina (EU276981)
Vibrio rotiferianus type strain LMG 21460T (AJ316187)
Clone sequence from the coral Oculina patagonica
Vibrio alginolyticus ATCC strain 17749 (X56576)
VC10 Acropora, Favites, Orbicella, Oculina, Pocillopora (19)
Vibrio (61)
Vibrio natriegens ATCC strain 14048 (HM771343)
VC16 Acropora, Favites, Pocillopora (5)
VC17 Host genera unrecorded (6)
Isolate sequence from the coral Fungia echinata (JQ409372)
VC18 Host genera unrecorded (4)
Isolate sequence from the coral Acropora hyacinthus (GU903236)
Vibrio (17)
VC20 Acropora, Pocillopora (6)
Clone sequence from the coral Acropora tenuis (GU184362)
VC22 Orbicella (37)
VC23 Fungia, Orbicella (6)
Clone sequence from the coral Orbicella faveolata (EU517640)
VC21 Dendronephytha, Orbicella, Oculina, Turbinaria (34)
Vibrio chagasii strain R-3712 (AJ316199)
Clone sequence from the coral Oculina patagonica
Vibrio crassostreae strain CAIM 1405 (EF094887)
Clone sequence from the coral Acropora eurystoma (GU319758)
Isolate sequence from the coral Fungia echinata (JQ409371)
Clone sequence from the coral Mussismilia hispida (GU199894)
VC24 Platygyra (3)
SCTLD-enriched ASV96
Isolate sequence from the coral Lophelia pertusa (HQ640863)
SCTLD-enriched ASV67
Unpublished clone sequence from coral with white plague disease
Vibrio pectenicida strain LMG 19642 (JN039139)
Vibrio orientalis ATCC strain 33934 (ACZV01000001)
VC25 Acropora, Montipora (7)
Vibrio tubiashii group (19)
Clone sequence from the coral Platygyra carnosus (JF411528)
VC26 Montipora, Oculina, Pachyseris, Platygyra (7)
Vibrio coralliilyticus ATCC strain BAA-450 (JN039154)
Vibrio sp. PaD1.27
Vibrio coralliilyticus ATCC strain BAA-450 (ACZV01000012)
VC27 Acropora (4)
Vibrio furnissii strain CIP 102972 (ACZP01000018)
Clone sequence from the coral Porites astreoides (JN694921)
Vibrio hepatarius type strain LMG 20362T (AJ345063)
Clone sequence from the coral Acropora tenuis (GU184499)
VC30 Acropora (21)
VC31 Dendronephthya (6)
Isolate sequence from the coral Acropora millepora (JN119271)
Vibrio strain LS12 (EF584071)
VC32 Vibrio brasiliensis group (5)
Vibrio (19)
SCTLD-enriched ASV25
Isolate sequence from the coral Acropora millepora (JN119269)
Vibrio strain LMG 19970 (AJ316206)
Vibrio superstes (AY155585)
Vibrio (18)
to outgroups
Photobacterium (82)
Enterovibrio(17)
Grimontia (17)
Salinivibrio (15)
Photobacterium (7)
0.10
≥90% Bootstrap
≥75% Bootstrap
SCTLD-associated ASV
Type Strain
Clone or Isolate sequence

1014

Fig. S11. Bioindicator *Vibrio* ASVs from the present study and a recent study related to *Vibrio* pathogens, type strains, and sequences obtained from the Coral Microbiome Database. Maximum likelihood and bootstrapped phylogenetic tree was produced using RAxML based on long (>1200 bp) sequences only, with the shorter coral associated sequences (dashed lines) and SCLTD-associated sequences (blue text) added using the Quick-add Parsimony tool in ARB. Colors represent qualitative information about the sequences as follows: Blue = SCTLD-associated ASVs from the present or previous study (Meyer *et al.*, 2019), Black bold = bacterial type strains, Black = clone or bacterial isolate/strain sequences. GenBank accession numbers are located in parentheses following each taxa label, when available. Circles at node represent bootstrap values of ≥ 90% (filled-in circle) or ≥ 75% (empty circle). Bar indicates 10% sequence divergence. Tree was rooted with *Thalassospira xianhensis* (EU017546) and *Thalassospira tepidiphila* (AB265822).

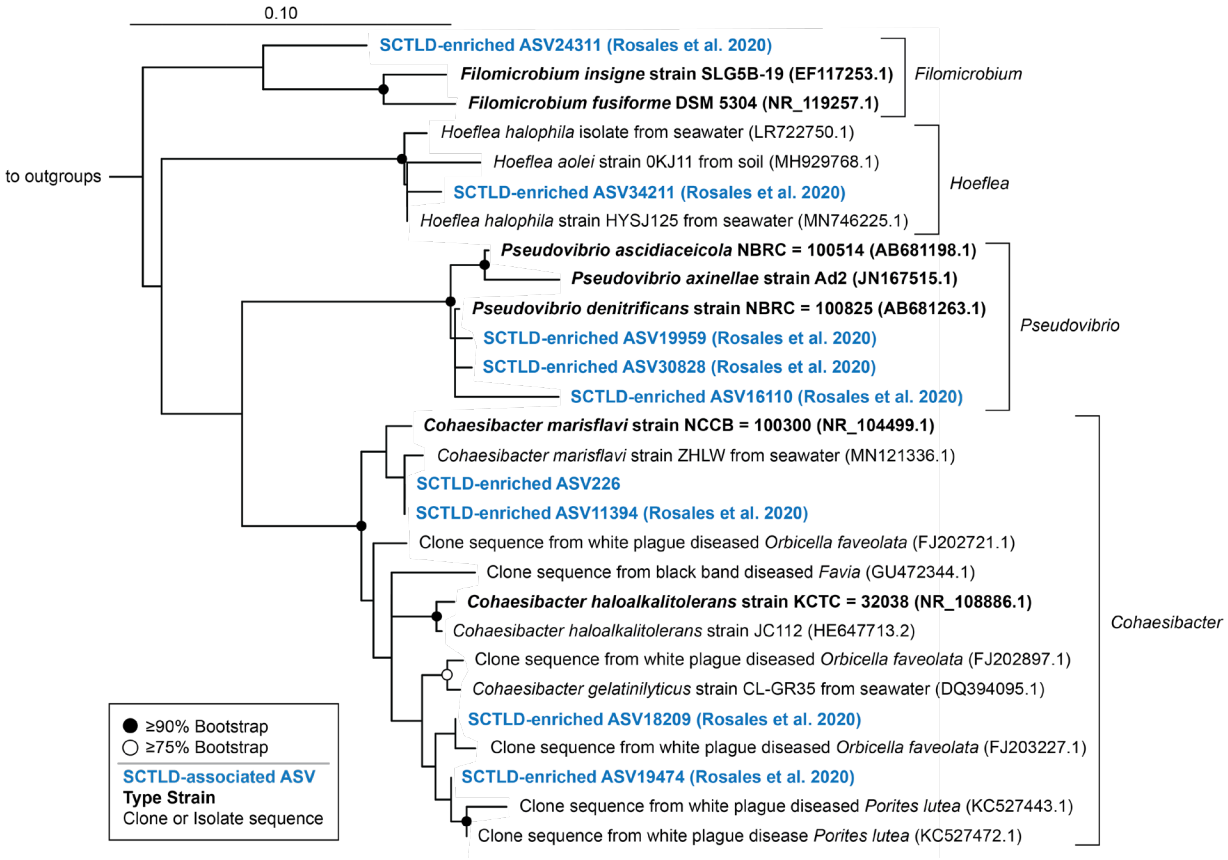

Fig. S12. One SCTLD bioindicator Rhizobiaceae ASV from the present study and several from a previous study related to other Rhizobiaceae sequences associated with corals and coral diseases. Reference phylogenetic tree was produced using RAxML rapid bootstrapping with an automatic bootstrapping approach to produce the highest-scoring maximum likelihood tree using only longer-length sequences (black). SCTLD-associated ASVs (blue) identified by differential abundance analysis or in a previous study (Rosales *et al.*, 2020) were added to the tree using the Evolutionary Placement Algorithm in RAxML. Colors represent qualitative information about the sequences as follows: Blue = SCTLD-associated ASVs from the present or a previous study (Rosales *et al.*, 2020), Black bold = bacterial type strains, Black = clone or bacterial isolate/strain sequences. GenBank accession numbers are located in parentheses following each taxa label. Circles at node represent bootstrap values of ≥ 90% (filled-in circle) or

≥ 75% (empty circle). Bar indicates 10% sequence divergence. Tree was rooted using the 16S rRNA gene of *Streptococcus mutans* strain ATCC 25175 (NR_115733.1).

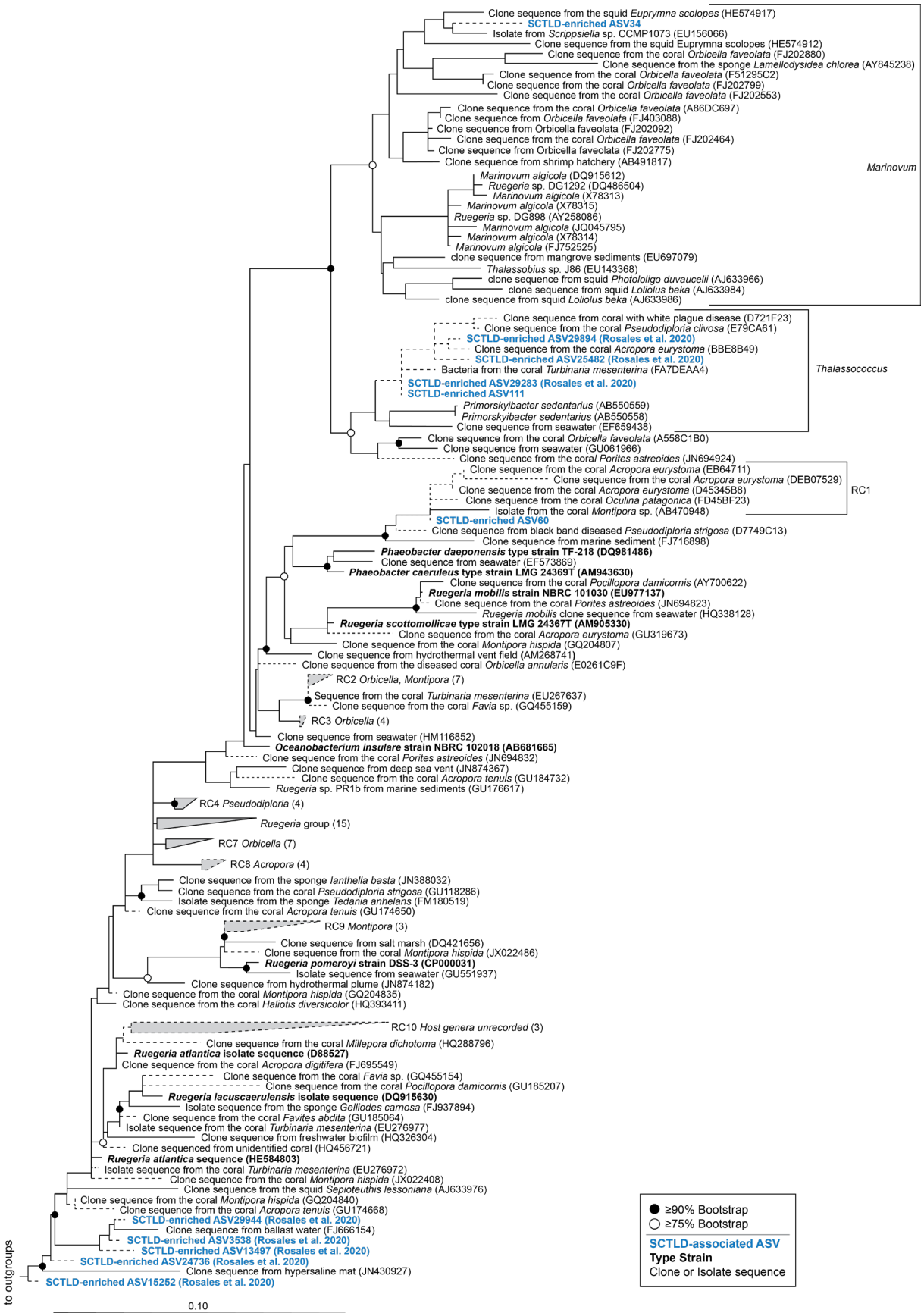
Clone sequence from the squid Euprymna scolopes (HE574917)
SCTLD-enriched ASV34
Isolate from Scrippsiella sp. CCMP1073 (EU156066)
Clone sequence from the squid Euprymna scolopes (HE574912)
Clone sequence from the coral Orbicella faveolata (FJ202880)
Clone sequence from the sponge Lamellodysidea chlorea (AY845238)
Clone sequence from the coral Orbicella faveolata (F51295C2)
Clone sequence from the coral Orbicella faveolata (FJ202799)
Clone sequence from the coral Orbicella faveolata (FJ202553)
Clone sequence from the coral Orbicella faveolata (A86DC697)
Clone sequence from Orbicella faveolata (FJ403088)
Clone sequence from Orbicella faveolata (FJ202092)
Clone sequence from the coral Orbicella faveolata (FJ202464)
Clone sequence from Orbicella faveolata (FJ202775)
Clone sequence from shrimp hatchery (AB491817)
Marinovum algicola (DQ915612)
Ruegeria sp. DG1292 (DQ486504)
Marinovum algicola (X78313)
Marinovum algicola (X78315)
Ruegeria sp. DG898 (AY258086)
Marinovum algicola (JQ045795)
Marinovum algicola (X78314)
Marinovum algicola (FJ752525)
clone sequence from mangrove sediments (EU697079)
Thalassobius sp. J86 (EU143368)
clone sequence from squid Photololigo duvaucelii (AJ633966)
clone sequence from squid Loliolus beka (AJ633984)
clone sequence from squid Loliolus beka (AJ633986)
Marinovum
Clone sequence from coral with white plague disease (D721F23)
Clone sequence from the coral Pseudodiploria clivosa (E79CA61)
SCTLD-enriched ASV29894 (Rosales et al. 2020)
Clone sequence from the coral Acropora eurystoma (BBE8B49)
SCTLD-enriched ASV25482 (Rosales et al. 2020)
Bacteria from the coral Turbinaria mesenterina (FA7DEAA4)
SCTLD-enriched ASV29283 (Rosales et al. 2020)
SCTLD-enriched ASV111
Primorskyibacter sedentarius (AB550559)
Primorskyibacter sedentarius (AB550558)
Clone sequence from seawater (EF659438)
Thalassococcus
Clone sequence from the coral Orbicella faveolata (A558C1B0)
Clone sequence from seawater (GU061966)
Clone sequence from the coral Porites astreoides (JN694924)
Clone sequence from the coral Acropora eurystoma (EB64711)
Clone sequence from the coral Acropora eurystoma (DEB07529)
Clone sequence from the coral Acropora eurystoma (D45345B8)
Clone sequence from the coral Oculina patagonica (FD45BF23)
Isolate from the coral Montipora sp. (AB470948)
RC1
SCTLD-enriched ASV60
Clone sequence from black band diseased Pseudodiploria strigosa (D7749C13)
Clone sequence from marine sediment (FJ716898)
Phaeobacter daeponensis type strain TF-218 (DQ981486)
Clone sequence from seawater (EF573869)
Phaeobacter caeruleus type strain LMG 24369T (AM943630)
Clone sequence from the coral Pocillopora damicornis (AY700622)
Ruegeria mobilis strain NBRC 101030 (EU977137)
Clone sequence from the coral Porites astreoides (JN694823)
Ruegeria mobilis clone sequence from seawater (HQ338128)
Ruegeria scottomollicae type strain LMG 24367T (AM905330)
Clone sequence from the coral Acropora eurystoma (GU319673)
Clone sequence from the coral Montipora hispida (GQ204807)
Clone sequence from hydrothermal vent field (AM268741)
Clone sequence from the diseased coral Orbicella annularis (E0261C9F)
RC2 Orbicella, Montipora (7)
Sequence from the coral Turbinaria mesenterina (EU267637)
Clone sequence from the coral Favia sp. (GQ455159)
RC3 Orbicella (4)
Clone sequence from seawater (HM116852)
Oceanobacterium insulare strain NBRC 102018 (AB681665)
Clone sequence from the coral Porites astreoides (JN694832)
Clone sequence from deep sea vent (JN874367)
Clone sequence from the coral Acropora tenuis (GU184732)
Ruegeria sp. PR1b from marine sediments (GU176617)
RC4 Pseudodiploria (4)
Ruegeria group (15)
RC7 Orbicella (7)
RC8 Acropora (4)
Clone sequence from the sponge Ianthella basta (JN388032)
Clone sequence from the coral Pseudodiploria strigosa (GU118286)
Isolate sequence from the sponge Tedania anhelans (FM180519)
Clone sequence from the coral Acropora tenuis (GU174650)
RC9 Montipora (3)
Clone sequence from salt marsh (DQ421656)
Clone sequence from the coral Montipora hispida (JX022486)
Ruegeria pomeroyi strain DSS-3 (CP000031)
Isolate sequence from seawater (GU551937)
Clone sequence from hydrothermal plume (JN874182)
Clone sequence from the coral Montipora hispida (GQ204835)
Clone sequence from the coral Haliotis diversicolor (HQ393411)
RC10 Host genera unrecorded (3)
Clone sequence from the coral Millepora dichotoma (HQ288796)
Ruegeria atlantica isolate sequence (D88527)
Clone sequence from the coral Acropora digitifera (FJ695549)
Clone sequence from the coral Favia sp. (GQ455154)
Clone sequence from the coral Pocillopora damicornis (GU185207)
Ruegeria lacuscaerulensis isolate sequence (DQ915630)
Isolate sequence from the sponge Gelliodes carnosa (FJ937894)
Clone sequence from the coral Favites abdita (GU185064)
Isolate sequence from the coral Turbinaria mesenterina (EU276977)
Clone sequence from freshwater biofilm (HQ326304)
Clone sequenced from unidentified coral (HQ456721)
Ruegeria atlantica sequence (HE584803)
Isolate sequence from the coral Turbinaria mesenterina (EU276972)
Clone sequence from the coral Montipora hispida (JX022408)
Clone sequence from the squid Sepioteuthis lessoniana (AJ633976)
Clone sequence from the coral Montipora hispida (GQ204840)
Clone sequence from the coral Acropora tenuis (GU174668)
SCTLD-enriched ASV29944 (Rosales et al. 2020)
Clone sequence from ballast water (FJ666154)
SCTLD-enriched ASV3538 (Rosales et al. 2020)
SCTLD-enriched ASV13497 (Rosales et al. 2020)
SCTLD-enriched ASV24736 (Rosales et al. 2020)
Clone sequence from hypersaline mat (JN430927)
SCTLD-enriched ASV15252 (Rosales et al. 2020)
to outgroups
0.10
≥90% Bootstrap
≥75% Bootstrap
SCTLD-associated ASV
Type Strain
Clone or Isolate sequence

1041

Fig. S13. Two SCTLD bioindicator Rhodobacteraceae ASVs from the present study and several from a previous study related to sequences from the Coral Microbiome Database encompassing several genera within the Rhodobacteraceae Family. Maximum likelihood and bootstrapped phylogenetic tree was produced using RAxML based on long (>1200 bp) sequences only, with the shorter coral associated sequences (dashed lines) and SCLTD-associated sequences (blue text) added using the Quick-add Parsimony tool in ARB. Colors represent qualitative information about the sequences as follows: Blue = SCTLD-associated ASVs from the present or a previous study (Rosales *et al.*, 2020), Black bold = bacterial type strains, Black = clone or bacterial isolate/strain sequences. GenBank accession numbers are located in parentheses following each taxa label, when available. Circles at node represent bootstrap values of ≥ 90% (filled-in circle) or ≥ 75% (empty circle). Bar indicates 10% sequence divergence. Tree was rooted with *Alteromonas* (AACY023784545) and *Methylophilaceae* (HM856564 and EU795249).